



Physical Root-Soil Interactions

Evelyne Kolb, Valérie Legué, Marie-Béatrice Bogeat-Triboulot

► To cite this version:

Evelyne Kolb, Valérie Legué, Marie-Béatrice Bogeat-Triboulot. Physical Root-Soil Interactions. *Physical Biology*, 2017, 14 (6), 25 p. 10.1088/1478-3975/aa90dd . hal-01609984

HAL Id: hal-01609984

<https://uca.hal.science/hal-01609984>

Submitted on 4 Oct 2017

HAL is a multi-disciplinary open access archive for the deposit and dissemination of scientific research documents, whether they are published or not. The documents may come from teaching and research institutions in France or abroad, or from public or private research centers.

L'archive ouverte pluridisciplinaire **HAL**, est destinée au dépôt et à la diffusion de documents scientifiques de niveau recherche, publiés ou non, émanant des établissements d'enseignement et de recherche français ou étrangers, des laboratoires publics ou privés.

Physical Root-Soil Interactions

Evelyne Kolb¹, Valérie Legué², Marie-Béatrice Bogeat-Triboulot³

1. PMMH, UMR CNRS 7636, ESPCI Paris, PSL Research University, Sorbonne Université - UPMC, Univ. Paris 06, Univ. Paris 07, 10 rue Vauquelin, 75005 Paris, France

2. Université Clermont Auvergne, INRA, PIAF, 63000 Clermont-Ferrand, France

3. EEF, INRA, Université de Lorraine, 54280, Champenoux, France

E-mail: evelyne.kolb@upmc.fr

Keywords: Plant root, mechanical stress, impeding soil, buckling, turgor pressure, root growth

Abstract. Plant root system development is highly modulated by the physical properties of the soil and especially by its mechanical resistance to penetration. The interplay between the mechanical stresses exerted by the soil and root growth is of particular interest for many communities, in agronomy and soil science as well as in biomechanics and plant morphogenesis. In contrast to aerial organs, roots apices must exert a growth pressure to penetrate strong soils and reorient their growth trajectory to cope with obstacles like stones or hardpans or to follow the tortuous paths of the soil porosity. In this review, we present the main macroscopic investigations of soil-root physical interactions in the field and combine them with simple mechanistic modeling derived from model experiments at the scale of the individual root apex.

Introduction

Roots absorb the water and mineral nutrients of the soil required by the shoot. Roots also assure the anchorage of the plant in the soil and provide a stable basis for the shoot emergence. Though interdependent, roots and shoots of the same plant organism live in dramatically different habitats. Responsiveness to change in environmental cues, called developmental plasticity, is markedly large for roots [1]. Root system development is genetically controlled by endogenous rhythms but it is highly modulated by the biological (competition and symbiosis with other organisms), chemical (nutrient availability, oxygen supply, pH...) and physical properties of its environment. The architecture of the root system, that is its three-dimensional shape, largely derives from the distribution and diversity of individual root apical meristems [2], which continuously sense and adjust their growth according to their local environment [3]. In addition, the formation of lateral roots also contributes strongly in shaping root systems and impacts soil resources capture [4].

Under non-stressful biological and chemical conditions, the root trajectory depends highly on the mechanical strength of the soil and on the presence of obstacles at the root scale. In contrast to aerial organs, root apices must exert a growth pressure to overcome the resistance to deformation of the surrounding soil and grow deeper or further into the soil. When experiencing a too large mechanical stress, radicles of seedlings have the ability to pass over stones, roots and other obstacles and deflect towards larger macropores. These intriguing and remarkable root capabilities were already mentioned by Charles and Francis Darwin in their book “The power of movements in plants” [5].

Since then, thorough and synthetic reviews and books in soil science and agronomy described the interplay between physical soil properties and root growth and architecture [6-10]. The aim of the present review is to combine these macroscopic approaches of the soil-root physical interaction with simple mechanistic modeling derived from model experiments at the scale of the individual root apex. The first part of this review summarizes the main characteristics of roots, root systems and soils. Then we describe their interrelationship through observations of the root response to growth in compact soils. The second part focuses on model experiments which tackle the different mechanisms involved in the response of the root apex to local mechanical stresses. In particular, root apices experience axial, radial as well as frictional stresses exerted by the soil. According to these different stresses and their relative contribution, roots respond differently and patterns of growth are modified. Root responses to mechanical stress including axial growth decrease, localized radial growth increase and reorientation of the growth direction will be addressed in three distinct parts. We provide simplified versions of the mechanisms involved and order of magnitudes rather than detailed values and more complex interpretations that can be found elsewhere.

1. Root-Soil mechanical interaction: a complex interplay between root and soil properties

1.1. Root system and root growth

Depending on plant species and age, a root system consists of different root types: primary or seminal root(s), adventitious roots and/or lateral roots. The primary or seminal root(s) are established during embryogenesis and emerge during seed germination. Adventitious roots develop on organs other than roots like leaf or stem. Lateral roots, formed post-embryonically on roots, usually constitute the bulk of the root system. Whatever its type and composition, the root system architecture is the result of growth of individual axes and of branching, that is lateral root emission [11]. Contrary to what happens in the stem apex, root growth and lateral root emission are processes located in two different zones of the root. The primary growth of the root (growth in length) occurs in the root apex while the primordia of lateral roots are formed from the pericycle layer and emerge in the mature zone of the root where growth no longer occurs (see Fig. 1).

The different root types share common anatomy and growth processes. The root apex, where primary growth occurs, can be divided into developmental zones: a meristem also called proliferation zone (including a transition zone), an elongation zone and a maturation zone (Fig. 1A). Root hairs are emitted in this maturation zone where cell elongation has stopped. Right at the tip of the meristem, the quiescent center, that is an organizational center, is surrounded by stem cells that divide and produce cells that proliferate in the meristem (Fig. 1D). Meristematic cells double in volume (called the cytosolic growth) before dividing. In the transition zone, cells leave the meristematic status and enter a phase of rapid elongation through vacuolization, that is an increase of the vacuole size. When rapid elongation stops, cells, having reached their mature size, enter the mature zone and differentiate. The cells issued from the stem cells are moved away from the quiescent center by the more recently produced cells, proliferating and then expanding, as a fountain. Thus, while the structure is relatively constant over time, the material is continuously renewed: cells flow from the meristem to the maturation zone [12]. The root apex is thus a dynamic system in which cells go through deep morphological and physiological changes [13]. Along the root apex, growth can be quantitatively described by the longitudinal strain rate. Kinematic analysis provides the velocity field (Fig. 1B) and its spatial derivative gives the strain rate field (Fig. 1C) [13, 14]. The strain rate issued from growth kinematics does not distinguish the cytosolic growth from the rapid expansion by vacuolization. In roots of eudicotyledon plants, a secondary growth may occur through the functioning of a secondary meristem, the cambium, in the radial direction, leading to woody roots. This second type of growth will not be considered in this review where we deal with penetration of soils by roots.

In the majority of plant species, the root meristematic zone is surrounded by a root cap [15, 16]. The root cap comprises a central region called columella and a lateral root cap located around it (Fig. 1F). The columella is made up of statocytes considered as the gravity sensing cells, in which there are starch-rich organelles called amyloplasts. In some plant species like *Arabidopsis thaliana*, the root cap extends far along the flanks of the root apex. Even though the size of the root cap is constant, this root tissue is continuously renewed. Close to the quiescent center, the root cap stem cells produce cells, that, after few divisions, progressively differentiate into columella or lateral cap cells. During their differentiation, the new cells push older cells toward the periphery which form peripheral cells. These cells acquire secretory functions, synthesize and export a high molecular weight polysaccharide mucilage, which forms a hydrated mass around the root tip. Some of these peripheral cells form specific secretory cells called border or border-like cells which slough off in the surrounding soil [17].

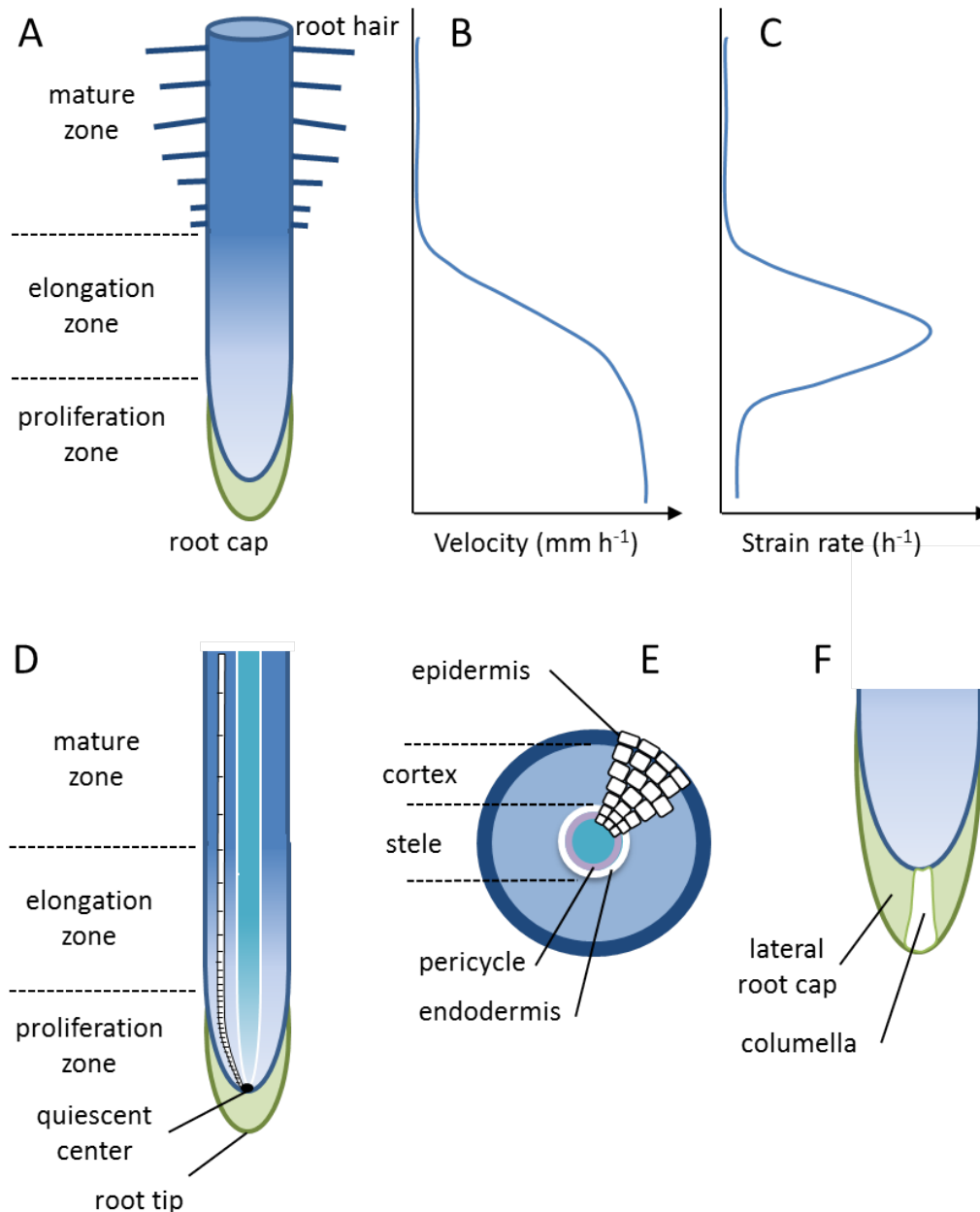


Fig. 1: Diagrams of a root apex. (A) The growing zone includes the proliferation zone (also called the meristem) and the elongation zone with the transition zone in between them. It is covered by a root cap. Root hairs grow only in the “mature” zone where there is no more elongation. The evolution of the velocity along the root apex in the reference frame of the immobile soil is shown by the colour gradient and in the graph (B). (C) Strain rate along the root apex. (D) Longitudinal section along the root apex showing a cell file, i.e. a sequence of cells, with the cell length increasing from the quiescent center to the mature zone. The stele that contains the conducting tissues (phloem and xylem) is symbolized in turquoise. Terminology about root tip and root apex depends on studies. Here the root tip is defined as the terminal end of the root, while the root apex corresponds to the growth zone, that is the root cap + the proliferation zone + the elongation zone. (E) Cross section showing the main tissues. (F) Detail of the root cap at the extremity of the root apex. The columella is made of statocytes that contain many starch-rich organelles and are thought to be gravity sensing cells. The lateral root cap covers a part of the proliferation zone. The peripheral root cap cells slough off while some are renewed as the root moves forward in the soil.

1.2. Diversity of soils and mechanical constraints

The root-foraging strategy depends on the nature of the soil or substrate, which results in various root architectures and physiological responses of plants. The rooting strategies will be different for roots growing on shallow soils over bedrocks or massive hardpans, deep loamy soils, artificial composts or even model substrates like vermiculite or agar gels [18, 19]. In addition to environmental cues like water or nutrients, changes in growth direction (tropisms) or in root system development (architectural features like lateral roots formation) depend on the mechanical stress field experienced by the root apices of the growing roots [20]. These stress fields are themselves a function of the soil or growth medium.

Natural soils are usually classified according to their texture, that is the relative proportion of clay (defined as the particles with equivalent diameters smaller than $2\ \mu\text{m}$), silt (particles between $2\ \mu\text{m}$ and $50\ \mu\text{m}$) and sand (particles between $50\ \mu\text{m}$ and $2\ \text{mm}$) independently of their chemical composition. Besides texture, soils scientists often consider “soil structure” as the spatial arrangement of the different components and properties of soil [21]. A typical volume of surface soil includes about 50% solids, mostly soil particles (45%), and organic matter (generally $< 5\%$) and about 50% pore space [22]. The soil pores are filled with gas (air) or liquid (water) or both, and are classified into channels, fissures and packing pores according to their shape in cross-section [19]. Voids, pores, cracks or crevices can already be present in the soil or produced by tillage, earthworm galleries or former decaying roots [23].

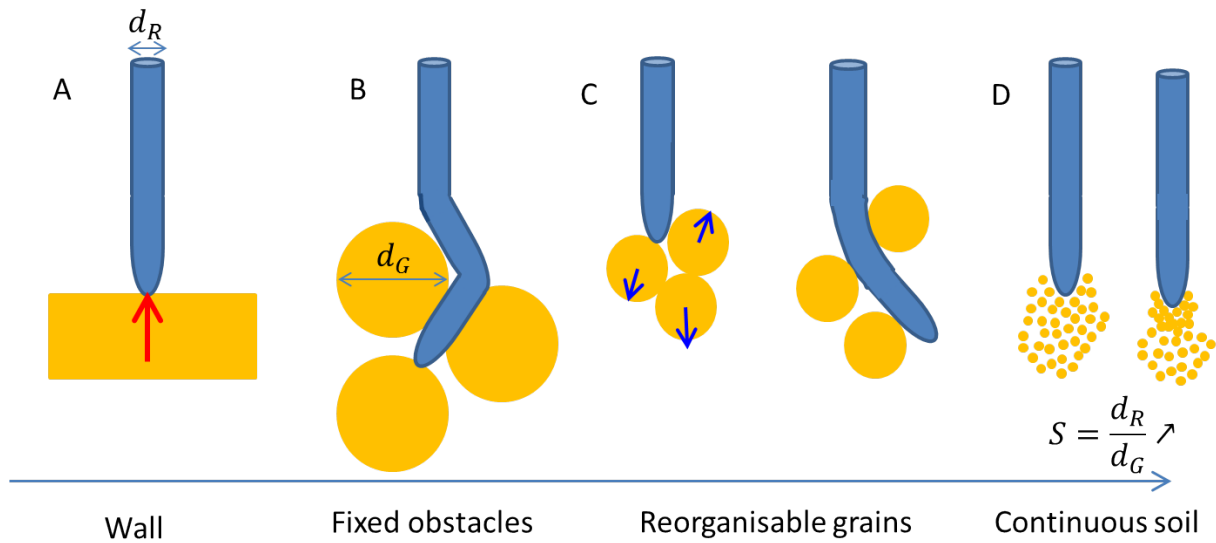


Fig. 2: Schematic diagram of the effect of the size aspect ratio S between root's diameter and typical length scale of soil heterogeneity on the mechanical stress experienced by the growing root.

When dealing with roots, the natural length scale is the root diameter (d_R) which should be compared with the scale of the soil heterogeneity (d_G) (**Fig. 2**). From a mechanical and geometrical point of view in natural soils, the large scale heterogeneities arise from physical barriers to root growth like stones or rocks (impenetrable obstacles), hardpans or surface crusts created by rainfall impact [18] (**Fig. 2A**). At a smaller length scale, roots may encounter clods ($d_G > 25\ \text{mm}$) that result from compaction by agricultural machinery or peds that are delineated by desiccation cracks in a shrinking soil [21]. As the rigidity of clods is large compared with that of the root and as the aspect ratio $S = \frac{d_R}{d_G}$ is small, roots cannot deform nor dislodge these large particles which behave like fixed obstacles (**Fig. 2B**). To be able to grow in this case, roots must exploit the complementary porous network and reorient their growth trajectory. For larger S values, when the size of the soil heterogeneity begins to be comparable

to the root scale, the soil particles are typically aggregates ($d_G > 250 \mu\text{m}$) formed by wetting and drying cycles [24] or sand particles, that act as movable obstacles for the root trajectory (**Fig. 2C**). In this case, the complexity of the root-soil interaction results from the granular nature of the soil at the root scale and the interplay with the growth trajectory. Root penetration induces reorganizations of the particles which in turn modify the distribution of pores and the local soil packing fraction, and affect the further root growth that may reorient [25]. This leads to an interesting feedback between root path and soil particle reorganization which has only begun to be quantified [26, 27] or simulated [28]. Eventually, for the largest S values, the soil particles are much smaller than the root diameter and there is no pore of sufficient volume into which the root can enter. Thus the penetration of the root is associated to a displacement of particles around the root apex and to a compaction of the soil (**Fig. 2D**). When there is furthermore not much spatial variability in the particle mechanical properties, soil will be considered as homogeneous or “unstructured” and is usually modelled as a continuous medium in finite element analysis with different stress-strain relationships [29, 30].

Homogeneous soils

When there are no continuous pores of sufficiently large diameter, soils will be considered as a continuous medium with a given soil strength, as the root tip must exert a force to deform or break the soil. The common way to quantify the mechanical strength of these homogeneous soils (unstructured soils) is to use penetrometry measurements, which is currently the best method for estimating the mechanical resistance to root growth [31].

Most penetrometers consist of a metal probe with a conical tip attached to a cylindrical shaft [32]. The probe diameter ranges from about 0.1 mm for a small needle penetrometer to over 10 mm for a large field penetrometer but it is usually of the order of 1 mm, which is comparable to the diameter of numerous crop roots like maize or peas. A relieved shaft with a diameter less than that of the cone basis is often used for limiting friction and adhesion between the soil and the shaft. Ideally the probe should be pushed into the soil at a velocity comparable to the root growth velocity (1 cm per day or equivalently around 10 microns per min) but for practical reasons, the probe penetration velocity is much faster, around 1 mm/min, and is typically between 50 and 600 times faster than the maximum rate of root extension. The force needed to push the penetrometer probe inside the soil at a constant velocity is measured and divided by the cross-sectional area of the penetrometer cone to obtain the soil strength. The range of soil strength obtained in this way is of the order of 1 MPa but depends highly on parameters like the soil bulk density and the moisture content. The increase in soil strength, also called “mechanical impedance”, results from the effects of both soil drying and soil compaction and sometimes it is difficult to decouple the two origins.

Soil compaction

The soil strength increases with soil bulk density. Agronomists usually refer to the dry soil bulk density, which is defined as the mass of dry soil divided by total soil volume. Soil strength increases with compaction, with soil bulk density ranging for example from 1.24 for loose soils to 1.38 for dense soils, up to 1.52 g/cm³ for very dense soils [30, 33]. The ability of soils to withstand compaction is affected by texture, clay mineral type, organic matter content and moisture content. The compaction of soils is due in part to external loads exerted by wheels under tractors or tillage machinery and by the trampling of animals [34]. Soil compaction might also result from climatic variations like heavy rainfalls that will impact soils and create a crust, or cycles of wetting/drying that modify the soil water content and promote the coalescence of soil aggregates [24].

The compaction of soil increases its average bulk density but also modifies the distribution of pore sizes. In particular, compaction decreases the number of coarser pores, alters the connectivity of the pore network and limits water uptake by roots [8]. This also limits solute transport, diffusion of

nutrients and gaseous exchanges (supply of oxygen and removal of carbon dioxide), which is detrimental for adequate soil aeration and for maintaining the soil microbiome activity and root growth.

Soil drying

While it is quite straightforward that soil compaction increases soil strength, another soil property, the water content, also strongly affects soil strength. The decrease of soil water content increases soil strength [6]. Consequently the observed mechanisms of root penetration will be completely different upon drying, the soil behavior varying from that of a brittle solid to that of a plastic-ductile material. Soils with low water content behave like brittle solids and can fracture under the compressive stress generated by the growing root as it advances through the soil [35]. On the other hand, soils with a high silty clay or organic content behave like plastics or liquids when they have a moderate water content: they will flow instead of crack when the compressive stress exerted by the root exceeds the yield stress of the soil. Depending on the water content, capillary bridges form between particles and induce tensile forces [36] that pull the aggregates toward each other and increase the typical size of soil heterogeneities. Water content on a percentage basis says little about the water available to plants because this depends on the soil nature and on the way water is distributed in the porous network. Soil scientists characterize the soil dryness using the soil matric potential (see **Box 1**) that represents the capillary and surface binding forces that affect water availability to plants [37]. The more negative the matric potential, the drier the soil, but the relationship is not linear and in relatively dry soils, a small decrease of water content strongly decreases the matric potential [38]. In many soils, a weak decrease of matric potential, keeping the water availability reasonable for the plants, induces a significant increase of the mechanical impedance. This leads to the conclusion that soil water deficit impacts root growth both by lowering the water availability and by increasing soil strength (see [6] for a review).

1.3. Effects of mechanical impedance on root growth and root system architecture

a) Root elongation and morphology

In field [39, 40] as well in lab experiments with soil compacted in a core [41, 42] or with pressure cells [43], root elongation rate (RER, as improperly called by biologists since it is a velocity, mm h^{-1}) varies inversely with soil strength. The measured soil strength depends on the tools and methods, leading to a large range of values and an apparent inconsistency. For instance maize RER was reduced by 50% for a penetrometer resistance ranging from 0.2 to 2 MPa depending on the study [41, 44, 45]. RER sensitivity to soil strength, that is the RER reduction relative to unconstrained state, seems to be species-specific. For instance, cotton and barley appeared to be more sensitive than pea and rice. A penetrometer resistance of 0.7-0.8 MPa decreased cotton and barley RER by 50%, while a resistance of 1 MPa decreased rice RER by 40%, and a resistance of 1.5 MPa decreased pea RER by 20% [41, 42, 44, 46, 47]. For all species, root elongation stops when soil strength becomes too high. According to Veen and Boone [45], in a wet soil, a maize root cannot overcome a penetration resistance of 4 MPa (extrapolated value) but it should be kept in mind that the resistance experienced by a root is 2.5 to 8 times lower than that measured by a penetrometer [6]. An important point is that RER reduction remains for a few days after removal of the stress, indicating that this change is not a simple mechanical effect but that acclimation through biological processes are involved in response to soil strength [46, 48-50] (see also part 2.1.c).

The reduction of RER is most often accompanied by an increase of the root diameter [39, 51, 52]. Root thickening concerns all root types (seminal, lateral, adventitious) and could be an advantage in terms of strong soil penetration (see part 2.2.c). Species with a higher root diameter, and those

showing a high increase in root diameter in response to strong soil are more efficient in penetrating strong layers [52, 53].

b) Root system architecture

While soil strength reduces RER of all root types, the elongation of lateral roots appears less sensitive to high soil strength than the primary roots of eucalyptus [54] or than the seminal roots of barley [55]. Main axes show higher diameter and elongation rate than secondary or tertiary roots. Thus, Thaler and Pages [56] suggested that higher sensitivity of the main axes to soil strength could be explained by higher frictions, which they supposed to be proportional to elongation rate. Or thinner roots might experience a weaker impedance because their diameter is more compatible with the size of the soil pores. In barley, an experience with ballotini (glass bead packings) of sufficient size to impede seminal roots but not laterals conducted to the doubling of the mean length of laterals [57]. This growth compensation by laterals was found in barley but not in wheat, highlighting species variability [55]. The reduction of main root axis elongation rate was sometimes accompanied by an increase in branching density [49, 56] but was not observed in other studies [55, 57]. This differential responsiveness of the root types to soil strength could lead to changes in root system architecture in response to uniform soil strength or hard pans. For instance, in the experiment mentioned above with barley in ballotini, the better development of lateral compared with seminal roots led to a denser superficial root system [57]. In a field with a compacted layer, the seminal roots of wheat explored the soil profile less efficiently [39]. Similarly, compaction reduced the final root depth of the pea root system more or less depending on cultivar but a high interaction between soil structure and climate impacting the depth of root system was highlighted [58]. Indeed, drought periods can produce vertical cracks that can be exploited by roots [40]. Soil strength, soil water potential and air-filled porosity interact and significantly affect root growth. Because all three are highly variable spatially and temporally in the field, it is difficult to predict root growth at the root system scale *in situ* [40].

2. Elementary mechanisms of root penetration inside soils

In the preceding part 1.3, we described the response of root growth and root system architecture to the mechanical impedance of soil or substrate. We now focus on model experiments aiming at explaining the elementary mechanisms of root penetration. Roots penetrate soil by growing and exerting axial and radial stresses (**Fig. 6**), which in the case of a homogeneous soil deforms it ahead of and around the root.

2.1. Root axial elongation as a motor for axial thrust in medium

We first deal with the mechanisms of axial pushing. The axial stress is called the growth pressure and is equal in magnitude to the pressure of the homogeneous soil, which opposes root growth [59]. The questions we address now are the determination of the maximum axial growth pressure of a root and its measurement.

a) Root growth pressure: measurements and range of values

Model experiments consist in measuring the axial force of a root against a force sensor (calibrated spring system, elastic beam, digital balance...). The first measurements of axial force generated by

growing roots were done by Pfeffer as earlier as 1893 [60] and reproduced long after by Gill *et al.* [61] and Souty [62], and more recently by using different techniques cited in Clark *et al.* [63].

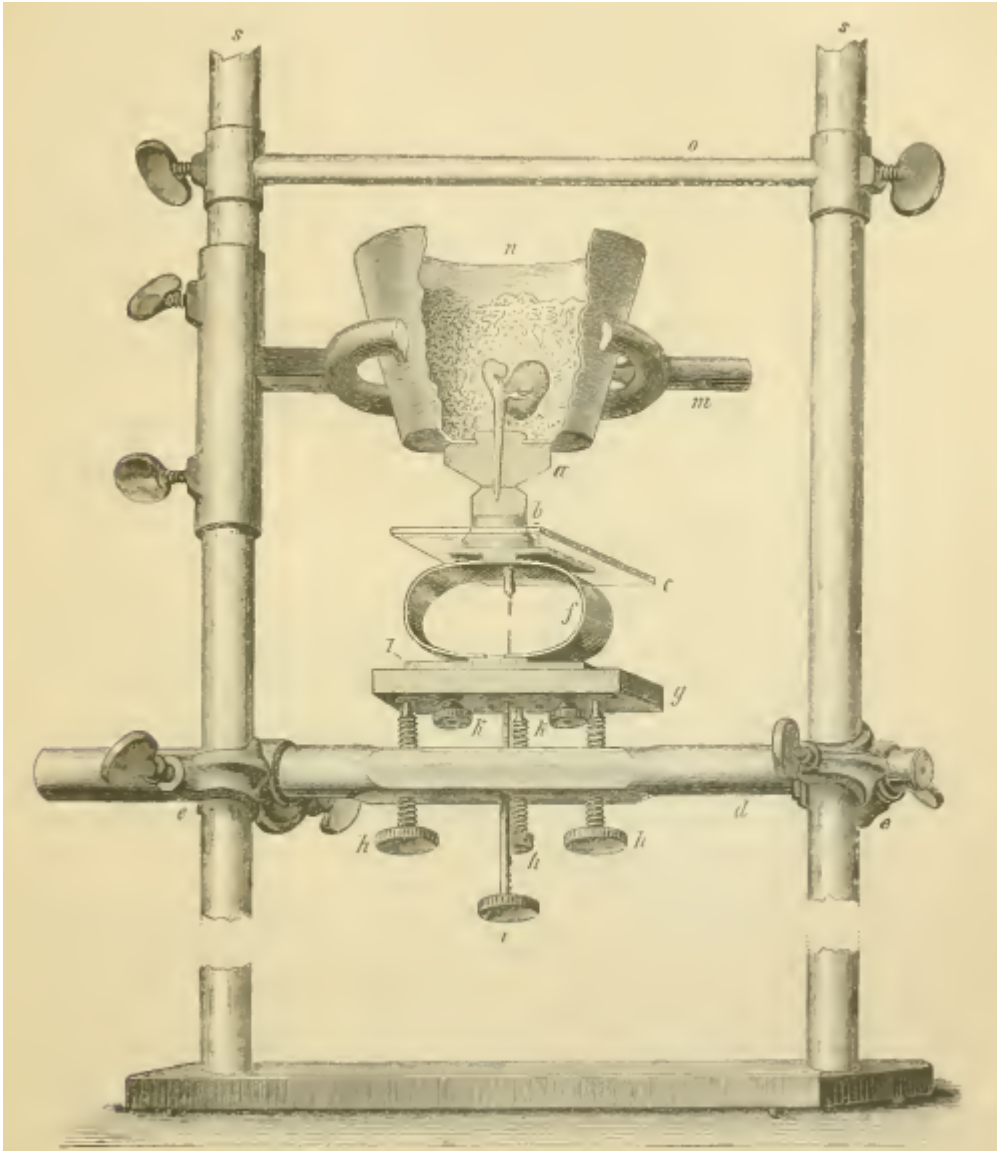


Fig. 3 : Experimental setup of Pfeffer [60] to measure the axial root growth pressure. The force measurement is performed through the deflection of the two curved elastic plates (f).

In most experiments the principle for determining the maximum root growth pressure is the following: The root tip is encased in a block (like a ceramic cone permanently saturated with water or a plaster of Paris) connected to a spring sensor of large stiffness, while the upper part of the root is guided into a tube or maintained laterally in a plaster block (plaster of Paris, dental plaster). The two blocks are independent and separated by a small air gap allowing the root growth. The deflection of the spring induced by the pushing of the root is followed as a function of time and then converted into a force. The typical force versus time curve usually presents 3 stages. The first one encompasses the phase of contact between the root and the sensor and a time delay during which the growth is reduced or stopped for a few minutes to hours. This can be attributed to a thigmomorphic response, that is a reduction of growth due to contact/compression (see part 2.3) [5, 64]. The second stage is characterized by a monotonic increase of the force with time over a period on the order of a few hours to one day. The last stage is saturation, when the root is fully impeded and cannot grow anymore. This threshold gives the value of the maximum penetrative force F_{Max} , which is an extensive value function

of the root size. In order to compare different species, a useful quantity is introduced, the maximum axial growth pressure σ_{Max} , which is an intensive quantity defined by:

$$\sigma_{Max} = \frac{F_{Max}}{S} = \frac{F_{Max}}{\pi d^2/4} \quad (1)$$

where S is the root cross-sectional area and d the root diameter. Depending on the experiment, the diameter is determined once the root has been removed from the setup under a microscope, or *in situ* by visualizing the root part in the gap.

Since the pioneering work of Pfeffer, various experimental systems have been proposed to measure the axial force a root is able to exert. The reported values for axial pressures obtained with the setup **Fig. 3** of Pfeffer were originally between 0.7 and 2.5 MPa for the seedlings tested (*Faba vulgaris*, *Zea mais* and *Vicia sativa*). In the work of Misra *et al.* [65], the axial root growth pressures were 0.5 MPa for pea, 0.29 MPa for cotton and 0.24 MPa for sunflower. A more detailed review of σ_{Max} values is given in Whalley *et al.* [66] and in Clark *et al.* [49]. Not surprisingly, the values for σ_{Max} are always of the order of the turgor pressure P , that is of the order of 0.1 - 1 MPa. We will come back to this later on.

In designing experimental systems for determining σ_{Max} , some care should be taken about possible artefacts. Limited diffusion of oxygen [67], inadequate water supply [6], or enhanced emission of ethylene [49] could be induced by the constraining material in which the upper part of the root or the root tip are maintained. In particular, ethylene might promote an increase in root diameter and a decrease in elongation rate, which will modify the value of σ_{Max} .

Most measurements of σ_{Max} reported in the literature have been for radicles of young non-photosynthesizing seedlings a few days old. The effect of seedling age has been investigated recently by Azam *et al.* [68]. By comparing primary roots of peas (2 - 3 days old) with lateral roots of tree seedlings (3 - 4 months old), they observed that the root growth pressures were surprisingly similar in the range 0.15 - 0.25 MPa. Misra *et al.* [69] had already shown that lateral roots and main root axis of pea had similar σ_{Max} .

Instead of pointing out the universality of the growth pressure values, most studies have focused on the slight differences observed in σ_{Max} values. The reason is that if roots of some species or different cultivars are able to generate greater values of σ_{Max} , they might better penetrate strong soils [53, 63], which would be a beneficial trait for selecting crops. For example, roots of dicotyledons (dicots) were observed to grow better in strong soil than those of monocotyledons (monocots). It has been suggested that this could be due to a greater value of σ_{Max} . But Clark [70] showed by using a shear beam force transducer method, that this does not seem to be the case, as the mean value of σ_{Max} for dicots (pea, lupin, sunflower) is 0.41 MPa, while the one for monocots (wheat, maize, barley and rice) is 0.44 MPa. Even in single species, values of σ_{Max} have been reported between 0.3 MPa and 1.3 MPa. Clark *et al.* [63] showed on pea seedlings that these differences mainly arise from measurement techniques rather than cultivars. They recommend experimental systems that allow root diameter to be measured *in situ*. Indeed when removed from the apparatus for observations under microscope, the root partially relaxes and its diameter shrinks, such that σ_{Max} will be overestimated. On the other hand, the gradual radial swelling that is observed for impeded roots (see part 2.2) could bias the determination of the root diameter, whose quadratic contribution in the formula (1) greatly modifies the value of σ_{Max} . Indeed, the exact protocol for determining the diameter entering formula (1) (location on the root, time to reach this diameter, way of impeding the root tip, stiffness of the force sensor...) should be specified for comparison.

b) Cellular origins of the root growth pressure

Root pressure allowing the penetration of the root into the soil is generated by root growth. In this part, we recall the main features and simplified models of root growth at the cell and organ scales and how the presence of a mechanical impedance is included in these models.

Root growth is mainly due to the expansion of cells within the elongation zone (**Fig. 1**). Indeed cell proliferation is essential for growth (providing new cells to the elongation zone) but most of the volume increase is due to cell expansion [71]. According to Lockhart [72], the relative expansion rate of a *single* cell depends mainly on turgor pressure (see **Box 1**), cell wall properties and membrane hydraulic conductivity (see the review of Geitman and Ortega [73] for more details). The membrane hydraulic conductivity is reasonably assumed to not limit cell expansion, so cell wall properties are considered as the main rheostat of cell expansion and turgor pressure is its driving force. The relative elongation rate or strain rate, $\dot{\epsilon}$, is thus given by (see **Box 2**):

$$\dot{\epsilon} = \phi \cdot (P - Y) \quad (2)$$

where P is cell turgor pressure and the parameters Y and ϕ denote cell wall properties that are actively regulated in response to environment. Y is a minimum threshold indicating that effective pressure must be high enough to allow cell wall extension and ϕ is the cell wall extensibility.

Understanding the biophysical control of root growth requires upscaling from cell to root. Along the root apex, $\dot{\epsilon}$ shows a bell-shaped profile (**Fig. 1C**), varying greatly from a few percent up to 35%, but cell turgor pressure is uniform over the growth zone [74]. Thus, as cells are moved along the growth zone -pushed by the new cells produced by the meristem- $\dot{\epsilon}$ variations must be controlled by changes in cell wall properties through changes of ϕ or Y . However the simplified Lockhart model still holds for the whole root (see Fig. 3 in [74] where the root growth velocity is observed to be an affine function of the turgor pressure), then the parameters Y and ϕ are averages of those of all cells or most probably of the fastest expanding cells along the root axis. In addition, in the radial direction, the root organ is made of concentric layers of different cell types that show different geometries and contribute differently to the mechanical properties of the root tissue. Indeed cell layers with extensible walls are connected to layers with less extensible walls. This generates compression and tension forces in addition to the local forces of turgor [75]. Using a multi-scale model built for the *Arabidopsis thaliana* root, Dyson *et al.* [76] showed that the epidermis has a more important influence on tissue-level growth parameters than other cell types and thus plays a predominant role in controlling root growth. This contradicts an older view where the internal tissues, inner cortex or endoderm, restrict root growth [74 and references therein]. Different plant model and root anatomy may explain this discrepancy. The measured Y and ϕ of a root section should correspond to those of the tissue layer that limits growth, whatever the tissue layer is.

Cell expansion is strongly anisotropic, generating the cylindrical shape to the root. As the cell elongates mainly in the axial direction, wall extensibility must be much larger in the axial direction than in the circumferential one [77]. Anisotropic cell expansion is attributed to its mechanical construction, the deposition of stiff aligned cellulose microfibrils perpendicular to the main axis of growth [78, 79], such that the cell wall is considered as an anisotropic fiber-reinforced composite material. Early, it was suggested that both the direction and the degree of anisotropic expansion could be controlled through the direction and the degree of microfibril alignment [80]. However some other control mechanisms may also exist [78]. For example, some *Arabidopsis* mutants exhibit higher radial expansion in root cells although there is no difference in microfibril alignment compared with the wild type [81]. In roots grown under water deficit, cells are more anisotropic but again no difference was observed in microfibril alignment [82]. Baskin [78] suggested that expansion rates in length and width are regulated by independent mechanisms. The microfibril length could also be involved in controlling

the radial expansion rate. In addition, at the organ scale, anisotropic expansion of some cell types may be controlled by the anisotropic expansion of other cell types in inner tissues. More recent studies of *Arabidopsis* roots [83] support the idea that cellulose microfibrils are deposited transversely to accommodate longitudinal cell expansion but are reoriented during expansion to generate a cell wall that is fortified against strain from any direction [83]. The orientation of microfibrils, as well as the mechanisms of cell wall loosening, are still intense research areas, in particular in developmental biology for understanding the link between morphogenesis and forces in tissues [84].

To model the biomechanics of a root in a resisting soil, Greacen and Oh [85] modified the Lockhart model to take into account the soil resistance σ . In the axial direction, the soil resistance acts against the effective pressure needed for axial growth and pushing, which results in a decay of the axial strain rate according to the equation:

$$\dot{\epsilon} = \phi \cdot (P - Y - \sigma) \quad (3)$$

In this equation, largely used by the community, the soil/root friction acting axially along the root flanks is omitted, assuming that this component is very small. Since the root-soil system is in equilibrium (quasi-static root growth), the axial force applied by the root equals the force opposed by the soil across the root cross-section. Thus the axial root growth pressure equals the soil resistance σ . It should be emphasized that P , ϕ and Y are not constants, but are physiological properties that are actively regulated. They change with root environment and soil resistance σ , as well as with the mechanical stress history of the root [86].

Box 1: The plant cell and its water potential

In contrast to animal cells, plant cells are surrounded by a rigid cell wall. In tissues, cell walls are cemented by a middle lamella, preventing cell migration. The outer boundary of each cell, the plasma membrane, separates the inside, called the cytoplasm, from the intercellular space called the apoplast. The plasma membrane is selectively permeable: water and small uncharged solutes cross it more readily than large or charged solutes.

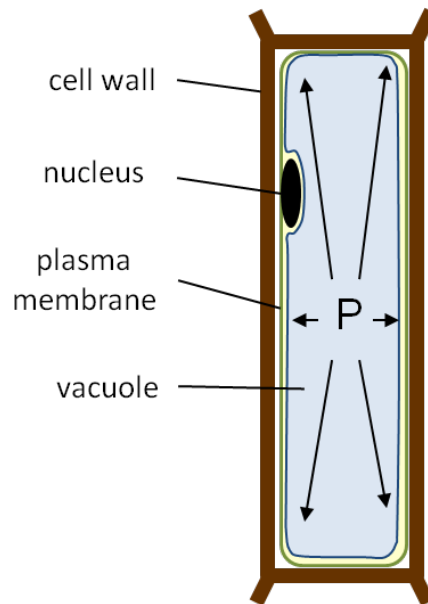


Fig. 4: Schematics of a plant cell. P is the turgor pressure acting isotropically.

Plant physiologists use the water potential, Ψ , defined as the chemical potential divided by the partial molar volume of water (free energy of water per unit volume) to quantify the water status. The water potential includes three components: $\Psi = \Psi_p + \Psi_\pi + \Psi_g$.

The gravitational component Ψ_g depicts the potential energy due to gravity: $\Psi_g = \rho_w g h$, where ρ_w is the density of water, g the acceleration due to gravity and h the height. When dealing with water transfer at the cell scale, Ψ_g can be neglected as compared to the two other components. Thus the cell water potential is $\Psi = \Psi_p + \Psi_\pi$.

The osmotic potential Ψ_π equals the opposite of the osmotic pressure Π ($\Psi_\pi = -\Pi$). It represents the interactions between dissolved solutes and water. The van't Hoff equation provides an estimate of the osmotic pressure for diluted solutions: $\Pi = RT \sum C_s$, where R is the gas constant, T the absolute temperature and $\sum C_s$ the sum of solute concentrations expressed in moles of osmotically active particles per cubic meter of water.

The hydrostatic potential Ψ_p , also called turgor pressure (P), is the hydrostatic pressure above atmospheric pressure [87].

As long as there is an imbalance of water potentials between the inside (ψ_i for the cell cytoplasm) and the outside (ψ_o for the external solution, soil or apoplast (cell walls and extracellular spaces)), there will be a water flow against the gradient of water potential. Thermodynamic equilibration results in $\psi_i = \psi_o$. Most plant cells live in a hypotonic environment, so the osmotic gradient $\Pi_i - \Pi_o > 0$ tends to drive water into the cytoplasm until $\psi_i = P - \Pi_i = \psi_o = -\Pi_o$. The cell wall prevents the cell from exploding and at equilibrium turgor pressure P balances the osmotic pressure gradient, i.e. $P = \Pi_i - \Pi_o$. Turgor pressure depends on cell type, ranging from 0.5 MPa in root cells to 2 MPa in leaf epidermal cells.

Box 2: The mechanical stresses in the cell wall and cell growth

The turgor pressure P causes the plasma membrane to press against the cell wall and generates tensile stresses in the cell wall. For a cylindrical cell, the hoop stress $\sigma_{\theta\theta}$ (which acts along the circumference of the cell wall) is twice the axial stress σ_{zz} (which acts along the long axis z of the cell which coincides with the root axis) [77]. Indeed, from the balance of forces, the magnitude of $\sigma_{\theta\theta}$ and σ_{zz} is directly related to the turgor pressure P by a geometrical amplification factor $\frac{R}{b}$ that depends on the thickness b of the cell wall and on the radius R of the cell (with $R \gg b$), such that:

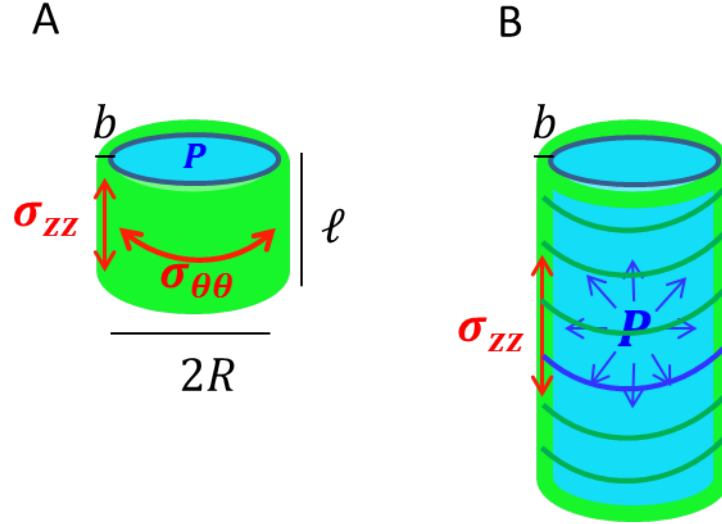
$$\sigma_{\theta\theta} = 2\sigma_{zz} = \frac{R}{b} \cdot P$$


Fig. 5: (A) Schematic diagram of a plant cell represented as a cylindrical shell of radius R , length ℓ and thickness b under internal pressure P . (B) Anisotropic growth of the cell when the axial stress in the cell wall exceeds the yield stress. The green circumferential curves represent the assumed orientation of the cellulose microfibrils in the cell wall for the simplest model of anisotropic growth.

These stresses induce strains in the cell wall (for the definition of stress and strain, see the review of Boudaoud [88]). The simplest rheological model (relationships between stress and strain) for the cell wall of a growing cell is a Bingham visco-plastic behavior, i.e. the cell wall deforms plastically above a yield stress σ_Y with a plastic viscosity η_P . Turgor pressure, the motor of expansion, is isotropic, but the cell walls are mechanically anisotropic (see the main text) and cells elongate mainly in the axial direction. Thus a cylindrical cell of length ℓ will grow when the axial stress in the cell wall exceeds the axial yield stress and the corresponding axial strain rate $\dot{\epsilon}$ (the relative variation of length ℓ with time t) will be:

$$\dot{\epsilon} = \frac{1}{\ell} \frac{d\ell}{dt} = \frac{\sigma_{zz} - \sigma_Y}{\eta_P}$$

In most papers, the strain rate of the cell is directly expressed as a function of the turgor pressure P and a pressure threshold Y . In the framework of the Bingham rheological model for the cell wall, Y is related to the yield stress σ_Y in the cell wall by $Y = \frac{2b}{R} \sigma_Y$, such that:

$$\dot{\epsilon} = \frac{1}{\ell} \frac{d\ell}{dt} = \frac{R}{2b} \cdot \frac{P - Y}{\eta_P}$$

which is simplified into:

$$\dot{\epsilon} = \phi \cdot (P - Y) \quad (2)$$

where $\phi = \frac{R}{2b \cdot \eta_P}$ is related to the irreversible axial wall extensibility and to the dimensions of the cell wall. The drawback of this concise formulation is that Y seems to play the same role as the isotropic turgor pressure P . Yet, Y is related to the cell wall yield stress σ_Y along the axial direction, but the directional information is hidden in the scalar equation (2).

c) What happens in response to strong soil?

In a strong soil, a root is completely impeded when the growth stops. According to equation (3), the condition $\dot{\epsilon} = 0$ gives an expression for the maximum axial growth pressure:

$$\sigma_{Max} = P - Y \quad (4)$$

Thus the turgor pressure P at the cell level gives the right order of magnitude of the maximum growth pressure σ_{Max} a root is able to exert in a soil.

When the root is partly impeded in a resisting soil (equation (3)), the root continues to grow ($\dot{\epsilon} > 0$) if $P - Y - \sigma$ remains positive. Increase in P or decrease in Y thus favor growth maintenance. There are several indirect or direct data showing that P increases in growing cells in response to impedance. Greacen and Oh [85] and Atwell [51] found an increase of the cell osmotic pressure in impeded roots. In these experiments, if the soil water potential was not affected by the impedance ($\psi_o = Cte$ - see **Box 1** for notations), the increased cell osmotic pressure ($\Pi_i \nearrow$) suggests an increase in turgor pressure ($P \nearrow$) such that the water potentials remain at equilibrium ($\psi_i = P - \Pi_i = \psi_o = Cte$). This osmoregulation, that could be achieved through cell internal metabolism or solute import, was interpreted as a consequence of the imbalance between phloem unloading (phloem is the tissue that conducts and delivers the solutes produced by aerial parts of the plants to the consuming sites) and reduced growth [51]. Osmotic pressure Π_i does not increase indefinitely in long lasting experiments, meaning that there are feedback regulations. Direct measurements of P in either completely or partially impeded pea roots confirmed the increase in cell turgor pressure in some cases [59, 89]. By contrast Atwell and Newsome [90] and Croser *et al.* [91] found no change in turgor pressure in impeded lupin and pea roots as compared to unimpeded roots. In these studies, cell turgor was measured on excavated roots and a relaxation of P after removal from the impeding soil cannot be ruled out. However it seems improbable since, in Clark *et al.*'s experiment [59], P remained constant for more than one hour after removal from the constraining ceramic block. Measurements of vacuolar osmotic pressure Π_i and turgor pressure P have shown that the water potential ψ_i of expanding cells was about 0.15 MPa lower in impeded roots compared to unimpeded roots. Assuming that P did not relax, this suggests that the apoplastic water potential ψ_o was lowered (see **Box 1**) and that the osmotic pressure of the apoplast Π_o was increased in impeded roots [91]. This supports the above mentioned hypothesis of imbalance between phloem unloading and solute retrieval by cells leading to an accumulation of solutes in the apoplast. All in all, P is either not affected or is increased by mechanical stress and thus is not involved in the growth reduction of impeded roots.

Following mechanical stress removal, cell osmotic pressure in the elongation zone of previously impeded roots returned to the control level in less than 12 hours [86]. Meanwhile growth rate required two to three days to recover [48, 50, 91]. If we consider that cell water relations were rapidly restored (return of the cell turgor pressure to the unimpeded state), this means that the cell wall mechanical

properties of elongating cells were durably affected. Focusing on the dynamics of root elongation rate following application (respectively removal) of mechanical stress, Bengough and McKenzie [92] highlighted a response in two steps: (i) a fast change occurring within 30 minutes that could be attributed to changes in effective turgor (so changes in P and/or Y) (ii) a slower and longer change that led to a new steady state of reduced (respectively increased) growth rate (after 15h). Rapid changes of cell wall properties were also shown in response to changes in water availability and were attributed to rapid changes of Y [93]. As seen before, P does not decrease in response to prolonged mechanical stress, thus the second phase of response can be attributed to further stiffening of the cell walls and/or effect of reduced proliferation rate (see below).

Kinematic analysis of durably impeded growth of roots showed that the growth rate reduction was due to a lower strain rate along the root and a shorter growth zone [46]. Cell length profiles established at 0, 24h and 48h after stress retrieval showed that the mature cell length was reduced under stress but gradually recovered and almost reached the length of the unimpeded level after 2 days [91]. This time lapse could correspond to the time necessary to fully renew the cells in the elongation zone and transition zone. The time a cell spends in the different zones along the root apex can be estimated by tracing its trajectory [12, 94]. Croser and co-workers [91] calculated that a cell needs 20h to cross the elongating zone of the unimpeded pea root. In poplar roots with a 10 mm-long growing zone, a cell needed 47h to cross the entire growing zone but spent 38h in the first two millimeters that include the apical meristem and transition zone [95]. The very low strain rate in this location makes the calculation of the time spent in it relatively inaccurate. In any case, the consistency between the time to renew cells in the transition and elongation zones and the time for the RER to recover after stress removal suggests that the potentiality of elongation of a cell could be acquired in this basal part of the meristem and is relatively independent of the environment during the fast expansion. This is in agreement with the idea that cells in the transition zone (**Box 1**) are quite sensitive to environment and receive their “growth fate” there [96].

A shorter elongation zone can be the direct consequence of shorter mature cells but also of a reduced cell production rate by the meristem, providing fewer cells to the elongation zone [71]. Coordination between changes of strain rate in the elongation zone and cell production rate has often been found. The meristematic cell production rate, that is also the cell flux in purely elongating zone, was decreased in impeded pea root [46]. Other studies also implied that the cell production rate was reduced by mechanical stress as nicely shown by Croser *et al.* [46]. Discrepancies with this tendency may come from an insufficient exposition time to stress and/or an insufficient level of stress. A lower cell production rate could be due to a longer cell cycle duration (due to lower cytosolic growth rate) and/or to less dividing cells (shorter meristem) [97]. Growth kinematics with sufficient accuracy within the meristem and longer experiments are required to better understand the response of proliferation to mechanical impedance.

d) How maximizing the thrust efficiency?

In the last section, we related the maximum growth pressure at the root level to the turgor pressure at the cell level through $\sigma_{Max} = P - Y$ by assuming there is no root/soil friction. However the thrust force (or pushing force) exerted by the growing part of the root to force its way has to overcome the soil resistance as well as the lateral friction due to the contact with the soil (**Fig. 6**). The friction involved here in the balance of forces is the one acting on the flanks of the root along the elongation and meristematic zones, where there is a differential motion between the root and the soil. In the following, we will briefly overview the works related to the contribution of the root/soil friction in the mechanisms of root penetration.

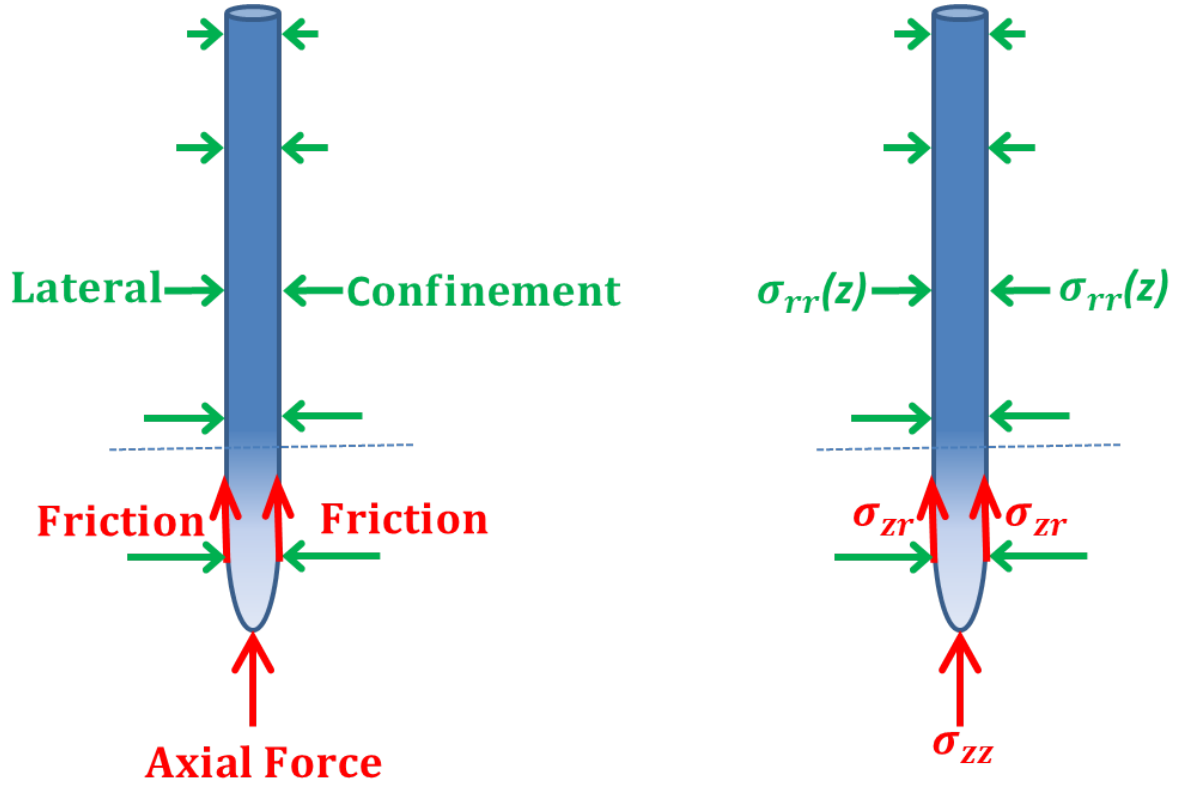


Fig.6: The red arrows represent the vertical forces (left panel) and corresponding stresses (right panel) exerted by the soil on the growing zone of the root apex aligned with the vertical z . The green arrows represent the lateral confinement along the radial axis r that might increase along the vertical due to the increase of the soil pressure with depth. The gradient of blue color indicates the location of the root growing zone and the dotted line delimits the elongation zone from the maturation zone, where there is no more motion of the root relative to the soil.

According to Bengough and McKenzie [86, 98], the resistances encountered by a root pushed into compacted soil cores were 2.5 times smaller than the ones encountered by a sharp penetrometer at the same rate of penetration ($2 \text{ mm} \cdot \text{min}^{-1}$), suggesting that less friction was experienced by the pushed roots. In addition, the resistances of growing roots were even smaller due to a combination of a smaller frictional resistance and a slower rate of penetration, as root growth velocity is of the order of $1 \text{ mm} \cdot \text{h}^{-1}$. McKenzie *et al.* [31] completed these works by using rotating penetrometer probe of similar dimension and rate penetration as for roots. By assuming a half-spheroid shape for the root tip, they inferred that the root-soil friction coefficient was $\mu = 0.21 - 0.26$, which is small but not negligible. The root cap is known to improve root penetration due to its tapering shape but also by the exudation of slimy mucilage (a polymeric gel) and the sloughing of the root cap border cells [17] that both line the root channel and contribute to limit soil/root frictions [86, 99]. Experiments compared the penetration of intact roots of maize with that of decapped ones [99]. When the root cap was removed, the elongation rate was about half that of intact roots and the diameter was 30% larger whilst growing in compact soils. The pushing force exerted by these roots was measured independently by placing the soil cores above a digital balance. The corresponding root penetration resistances were 0.31 MPa for intact roots and 0.52 MPa for decapped ones, suggesting that the growing decapped roots have to overcome a higher component of soil friction. Thus the mucilage and the release of border cells issued from the root cap are often viewed as a “lubricant” of the root-soil interface [100]. However the mechanisms underlying the improvement of root penetration by mucilages or other root exudates are still open questions [101]. The nature of the sheared zone at the root-soil interface might

change from a homogeneous solid to a granular heterogeneous medium, to a viscous liquid, or even to a more complex fluid, depending on the presence of mucilage and its degree of hydration [102]. Usually the frictional terms acting against the penetration of probes inside soils are measured by means of a penetrometer and interpreted as a solid-solid friction, i.e. it is assumed a Coulomb criterium that linearly relates the shear stress τ to the normal stress σ_{rr} at the interface by means of the soil-probe friction coefficient μ (see Fig. 6 for notation of stresses):

$$\tau = \sigma_{zr}(z) = \mu \sigma_{rr}(z) \quad (5)$$

Possibly a modified Coulomb criterium can be used to take into account the cohesion (c) due for example to the soil water suction exerted by capillary bridges at the soil particle-probe interface [36], i.e. $\tau = \sigma_{zr}(z) = \mu \sigma_{rr}(z) + c$.

The case of root penetration is however more complex. The released cells with the mucilage form a liquid and viscous boundary layer between the root and the soil [99] that modifies the mechanical and wetting properties of the narrow zone of soil immediately surrounding the roots [99]. Read *et al.* [103, 104] measured the surface tension and viscosity of mucilage collected from maize and lupin root seedlings grown on filter papers with different moisture content. In particular, they found that mucilage contains phospholipid surfactants that lower the surface tension (minimum value of 48 mN.m⁻¹ for filtered and concentrated mucilage) compared with that of pure water (72 mN.m⁻¹). Other studies have shown that after drying, mucilage becomes hydrophobic and limits the rewetting of the root-soil interface [105]. In any cases, mucilage modifies the wetting properties of the root-soil interface compared with the bulk soil. This might affect the way soil particles near the root apex are bound together by capillary bridges and therefore modify the typical size of soil aggregates along the root path, hence the root trajectory itself (see part 1.2). Moreover oscillatory rheological measurements have shown that the mucilage of axenic maize with its border cells behaves at low frequency (lower than 1 Hz) like a weak visco-elastic gel [106]. The authors suggest that due to this elastic contribution at the low shear rates, the movement of the root through the soil will draw soil particles in contact with the mucilage towards the root surface and help maintaining the root-soil contact.

A second feature that can improve straight penetration of roots is the firm holding of the non-growing part of the root inside soil. A large lateral confinement by the soil will help maintaining the root mature zone static while the root tip is growing. Indeed the confinement might provide a proportionally greater axial resisting force. However a rough estimation of the solid-solid friction force that might be involved at the root mature zone-soil interface indicates that its value for short emerging radicle is relatively low compared with the reaction force exerted by the growing zone. Then the anchorage of the seedling provided by the soil lateral confining pressure is too weak for small depths (see Box 3 for calculations of order of magnitudes).

Indeed a far more efficient anchorage for young seedlings is produced by the presence of root hairs in the root mature zone. In the work of Bengough *et al.* [107], hairless maize mutants were compared with their wild-type counterparts with hairs. The root tip anchorage was higher in the presence of root hairs and enabled better soil penetration. In particular the depth of penetration was larger for wild-type roots and the length of the root pushed-up above the soil surface was greater for the hairless mutant in the case of the loosest soils. Accordingly the pull-out forces required for extracting the roots of soil were larger for hairy roots than for hairless roots, the force being 13 times larger in the case of the loosest soils. Then the disrupted region of soil during pull-out was greater for hairy roots. In particular this region had a larger lateral extent radially away from the hairy roots with soil motions observed at up to four times the root radius, whereas the hairless mutant hardly disturbed the surrounding soil.

Box 3: Speculative estimation of the friction forces at the root-soil interface

The growing zone of a root exerts an upward reaction force (vertical red arrow in Fig. 7) on the non-growing zone. We take the case of a young seedling root with no laterals, the seed being just located at the top surface of the soil. The resisting forces acting against the up-lifting of the root are the weights of the root and aerial part (downward vertical black arrows) and the static friction forces at the non-growing part of the root-soil interface (orange arrows). These downward friction forces arise due to the upward force produced by the root's growing zone in the impeding soil. The confinement due to the lateral stress $\sigma_{rr}(z)$ acting on the flanks of the root determines the amplitude of the friction force along the mature zone of the root. Thus the maximum friction force $F_{friction}^{Max}$ before sliding, hence up-lifting, can be computed.

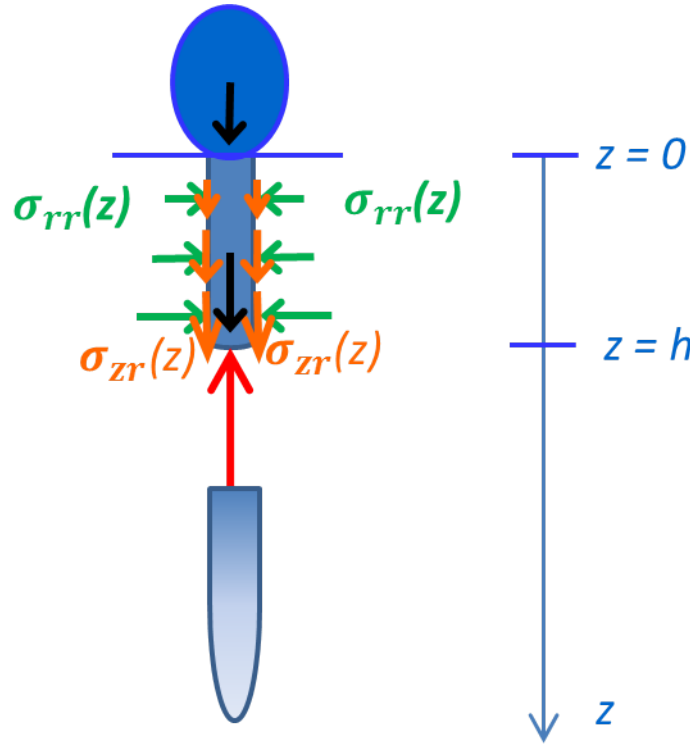


Fig.7: Schematic diagram of the forces resisting to the up-lifting of the root outside the soil due to growth in the constraining soil. The seedling is artificially decomposed into a growing part (bottom part) and a non-growing part (upper part) over which the balance of forces is made. The root axis z is aligned with gravity. The seed is just lying on the soil surface at $z=0$ and the non-growing part of the root is buried till the depth $z=h$.

For this calculation we don't take into account root hairs, mucilage or root cap cells that might modify the soil frictional properties at the root-soil interface. Thus we assume that the frictional stresses σ_{zr} are purely interfacial and related to the lateral confining stresses σ_{rr} by means of the usual Coulomb law (without any cohesion), that is $\sigma_{zr}^{Max} = \mu \sigma_{rr}$, where μ is the static coefficient of root-soil friction. The lateral confinement is itself related to the local vertical stress $\sigma_{zz}(z)$ that increases with depth z , i.e. $\sigma_{zr}^{Max}(z) = \mu \sigma_{rr}(z) = \mu K \sigma_{zz}(z) = \mu K \rho_S g z$ with K the lateral earth coefficient, ρ_S the density of the soil and g the acceleration of gravity. The corresponding friction force integrated over the length h of the non-growing part of the root inserted in soil will be $F_{friction}^{Max} = \pi \frac{d_R}{2} \mu K \rho_S g h^2$. A crude estimation by using $d_R = 1$ mm, $\rho_S = 2000$ kg.m⁻³, $\mu = 0.3$ [31] and $K \approx 1$ gives a maximum friction force of $F_{friction}^{Max} \approx 0.1$ N for a vertical anchored root length of $h = 10$ cm. As a comparison, the root weight over the same length will be $W_R = \rho_R g h \pi \frac{d_R^2}{4}$ where ρ_R is the root density, which gives

$W_R \approx 10^{-3} N$ for $\rho_R \approx 1000 \text{ kg.m}^{-3}$. The seed weight will be $W_{seed} = \rho_{seed} g \pi \frac{d_{seed}^3}{6}$, that is $W_{seed} \approx 10^{-2} N$ for a seed diameter d_{seed} up to ten times larger than the root diameter and a seed density ρ_{seed} of the order of the root density. Thus in this case of a root having already the length h with the seed at the soil surface (which is the case of the experiment of [107]), the friction force is the main resisting force contributing to the stabilization of the root against the pushing-up force F_{push} . By taking $F_{push} \approx \sigma_{Max} \times \frac{\pi d_R^2}{4}$ with $\sigma_{Max} = P - Y \approx 0.1 \text{ MPa}$, the maximum growth pressure defined in part 2.1.a, we obtain $F_{push} \approx 0.1 N$. This is the same order of magnitude as the maximal friction force due to anchorage along 10 cm depth. Alternatively these rough estimations provide a critical length of anchorage above which the root is stabilized against uplifting. Then according to these calculations, the root has to be sufficiently anchored, such that the length of the non-growing zone extends until a depth greater than h_{Lim} . In this way, $F_{friction}^{Max} = \pi \frac{d_R}{2} \mu K \rho_S g h_{Lim}^2$ is sufficient to overcome the up-lift force F_{push} . By taking $\sigma_{Max} \approx P$ in the expression of F_{push} , this gives $h_{Lim} = \sqrt{\frac{P d_R}{2 \mu K \rho_S g}}$ and we recover $h_{Lim} \approx 0.1 \text{ m} = 10 \text{ cm}$ for a root's diameter of $d_R = 1 \text{ mm}$. More generally we obtain that the critical length of anchorage h_{Lim} increases as the square root $\sqrt{d_R}$ of the root's diameter when the root-soil friction is purely interfacial and for the geometry described in [107]. Note that the scaling is different for emerging radicles initiated from a seed sowed at a given depth, then the yield stress and pressure of the soil above the seed has to be taken into account. And as gardeners say, the seed has to be sowed at a depth more or less equal to its diameter.

2.2. Radial thickening of the root

a) Macroscopic observations

Mechanical impedance commonly causes roots to become thicker [108]. The magnitude of the swelling for seminal roots of different plant species (dicots and monocots) has been observed to be smaller in field studies than in laboratory studies [53], probably because roots exploit the small scale variations in soil strength which exist in the field. Materechera *et al.* [53] observed that the roots which had higher thickening also had a higher percentage of penetration into the compacted subsoil below a tilled (non-compact) layer in a field study.

The thickening of the root seems to be localized near the apex in the expanding tissues [109]. This is clearly visible in the model experiment of Kuzeja *et al.* [110] where a computerized feedback-controlled device allowed applying a constant force at the root tip of a maize seedling. The recorded time-lapse images showed that the radial swelling was localized at about 3 mm behind the root cap for a root diameter of the order of 500 microns. Therefore it is probable that in model experiments and for large impedance, the radial thickening occurs in localized zones at a distance from the root tip, probably in the zone of rapid elongation where the volume increase of cells is the largest one.

b) Cellular observations of the root thickening

Radial thickening of the root can be due either to an increase of the number of cell layers or to an increase in cell diameter. A deep anatomical study focused on the changes induced by impedance on the size, shape and number of cells within the different tissue layers and along the barley root [108]. As already seen by Barley in maize [111], the number of cells in the stele and the cortex was slightly increased, due probably to more periclinal divisions in the apical meristem (divisions tangential to the root cylinder, generating more cell layers). However most of the increase in root diameter could be

attributed to the cell swelling in the outer cortex layers. Similarly, the increase of pea root diameter in response to impedance was mainly due to the swelling of cortex cells rather than to the increase in the number of cortical cell layers [46].

Cell maturation implies no more large changes of cell shape. Cell swelling should thus occur during expansion. Indeed, the diameter increase concerns the root section that has been rapidly expanding under impedance. For instance the root swelling was observed to extend over 5 mm in the elongation zone in the 6h hour experiment of Kuzeja *et al.* [110] and over 30 mm in the 7 day-long experiment of Wilson *et al.* [108], which length includes the elongation zone and some mature zone. It appears also that the swelling zone gets closer to the root tip as the root remains longer under stress, which is consistent with the shortening of the meristem.

In optimal conditions growth anisotropy of cells is controlled through the deposition of aligned cellulose microfibrils perpendicular to the main axis [77]. Experiments on pea root growing in a compacted soil layer before entering a loose soil layer showed that root diameter recovered to control level as soon as the root grew in the loose layer, whereas the root elongation rate remained reduced for several days [48]. This supports the idea suggested by Baskin [78] and mentioned before that the control of radial cell expansion (swelling) is different from that controlling expansion along the main axis.

c) Does root thickening optimize penetration?

Several hypotheses presenting the increase in root diameter as a mechanical advantage for root penetration into strong soils were raised up [112]. First, in an homogeneous soil considered as an elasto-plastic medium, finite-element analyses have shown that a radial increase of the root will relieve axial stress ahead of the root tip [113-115]. This mechanism which reduces the axial resisting pressure of the soil helps the root to continue to grow straight along its axis. The same mechanism also explains a possible tensile failure of the soil ahead of the tip and the creation of a crack in which the root tip could engage. In the case of gel substrates, root swelling will help opening and propagation of cracks in front of the root tip, in a way analogous to the burrowing of earthworms in muddy sediments [116], except for the peristaltic wave progression. In the work of Abdalla *et al.* [113], the same mechanism has been proposed for granular soils, although the calculations are initially based on the assumption of a continuous medium. Indeed, in a granular soil, this root diameter enlargement will open pores between grains and will facilitate the root entering into the gap. In all these cases, root thickening might induce soil cracks ahead of the root tip and/or release of pressure on the root tip, thus facilitating cell elongation and root growth [43, 113]. The cycle of reduced axial elongation, thickening near the root tip, relief of the axial stress, further root elongation, is repeated every time the root tip experiences a zone of larger impedance and the root proceeds to grow with a thickened section. The root cap being suspected to sense obstacles [50, 64], the release of pressure on the root cap could also limit the thigmomorphism response.

Another reason explaining the advantage of radial expansion for root's straight penetration is the better resistance of thicker roots to bending and buckling. Thus thick roots are supposed to penetrate hard layers more easily [117, 118]. For heterogeneous soil structures, buckling of the root can occur when the root tip is located at interfaces between pores and solid regions but also at interfaces between solid regions of different strengths [40]. Determining the buckling threshold is essential for knowing whether the root will penetrate further or being deflected in the case of hardly deformable soils. From a mechanical point of view, buckling is an elastic instability, i.e. a passive mechanism, producing a deflection of the root above a critical compression force acting along the longitudinal axis of the root.

In the case depicted in Fig. 8 where the root apex is growing in an air gap or a pore against a wall or a stiff soil (**Fig. 8**), the dimensional expression of the compression force F_B for which buckling occurs, scales like:

$$F_B = \alpha \frac{EI}{\ell^2} \quad (6)$$

E is the root Young's modulus that characterizes its rigidity, ℓ is the effective length along which the root is not supported, that is typically the length of the pore, and I is the moment of area that characterizes the way the root tissue is distributed over the cross-section. Thus I depends on the root geometry. For a simple object like an homogeneous plain cylinder of diameter d , the moment of area would be $I = \frac{\pi d^4}{64}$. and the correct non-dimensional prefactor α in eq. (6) could be explicitly given, depending on the way cylinder extremities are maintained (free, pinned, fixed...). For a complex system like a root with a conical shape at the tip, inhomogeneous, anisotropic and water-dependent mechanical properties, it is not worthy to go beyond a dimensional analysis. Therefore the buckling force of the root inside a pore can be rewritten as:

$$F_B \sim \frac{Ed^4}{\ell^2} \quad (7)$$

It means that for the same length ℓ , a thick root (with a large diameter d) will better resist to larger external forces before buckling, compared with thinner roots. According to Materechera *et al.* [52], roots of dicotyledons which are usually thicker compared with monocotyledons and expand radially to a greater extent are less prone to buckling.

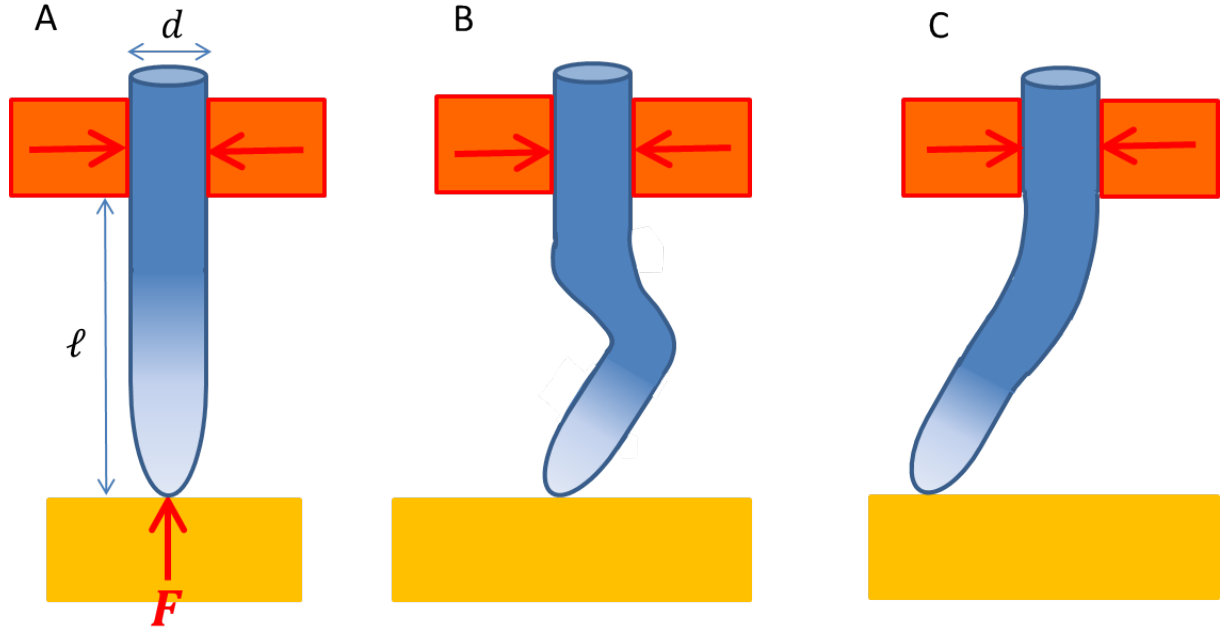


Fig.8: Buckling and bending phenomena for a root of diameter d whose extremity is not supported laterally over a length ℓ . As in Fig. 1, the root zone with the colour gradient represents the elongation zone. (A) The root growth against the wall creates a progressively increasing compression force F in the root (red vertical arrow). In this schematic drawing, the root is maintained laterally (upper orange blocks) at a distance ℓ from the root tip and is supposed to be pinned at the bottom interface. (B) When the compression force reaches the Euler threshold $F_B \sim \frac{Ed^4}{\ell^2}$, the root buckles. A first curvature is

generated and the maximal lateral shift of the root can be located outside the elongation zone. (C) As the root bends toward one side, the growth direction is reoriented.

d) Limitations of the radial expansion

Root radial thickening produced by axial stress can be observed if there is no lateral mechanical hindrance around the root elongation zone. This is probably the case in model experiments where the root can freely swell in the air gap between the two blocks maintaining the root extremities. Conversely the extent of the radial swelling will be limited by the degree of lateral confinement.

Few experiments have investigated the extreme case of root growing inside rigid pores. In the old experiment of Wiersum [119], seedlings of 17 species with root diameters ranging from 100 to 700 microns were grown in sintered glass-filter discs, i.e. a network of pores of fixed geometries between rigid and fixed particles. By *a posteriori* measuring the diameter of the roots that grew through the filter discs and of the ones that remained on the top, Wiersum concluded that primary and first order lateral roots were only able to penetrate pores that had a diameter exceeding that of the root. Unlike [119], Scholefield and Hall [120] observed the presence of roots of ryegrass in pores much smaller than their nominal thickness as long as the rigid pore diameter of steel meshes or glass capillaries was exceeding a critical size determined by the stele diameter. In the more recent review of Bengough *et al.* [86], it is briefly mentioned that roots can grow in even smaller pores than the stele diameter with a relative thinning of both the cortex and the stele of maize roots [2].

Different conclusions might arise depending on the value of root nominal diameter compared with the imposed constriction size. When the nominal diameter of the root is not known, it must be estimated from the diameter in the elongation zone of a hypothetical identical root which would not have experienced the constriction. At least, this requires measuring the diameter *in situ* for avoiding relaxation effect due to stress retrieval [121] when the root is extracted from the embedding soil or substrate. A further complication comes from a possible artefactual swelling due to uncontrolled axial force. As mentioned by [86], the large lateral confinement due to the constriction produces an important axial friction force acting against the root growth (Fig. 6). Thus, the constriction-induced stresses are not purely radial and this additional axial resistance could promote an extra swelling of the root. The determination of the nominal diameter can therefore be biased even if this diameter is measured *in situ* outside the constriction zone.

In very constrained situations, it is known that the cortex adapts to the geometry of the pore. Invaginations on roots grown in real soils are memories of the root passage inside pores. In the case of narrow rock fissures [122], the cortex is flattened with “wing-like” structures extending along the direction of the fissure, whereas the stele remains approximately cylindrical. Older roots can show constricted zones as a result of inhibited secondary growth in hard soil layers [123].

Wiersum [119] used the porosity of sand particle packings inside containers of different internal diameters to control what he called the “structural rigidity” of pores. In the narrower container, the mobility of sand particles was restricted and the root growth of *Avena* and *Brassica* seedlings reached smaller depths compared with the growth in wider container. Thus young roots could force their passage through pores of size smaller than their diameter as long as they could displace soil particles. These experiments point out the importance of considering the degree of jamming of soil particles and the corresponding confining stress in the root penetration [27]. In model experiments with static granular packings (sand particles, ballotini...), the transmission of forces through force chains and the friction at the walls lead to a screening of the pressure with depth for low aspect ratio of the container

(small width over height). Thus the proximity and mechanical properties of boundaries (friction and rigidity) could affect the pressure really experienced by the root. In granular packings, building-up and collapse of force chains [124-126], that are established between the penetrating object and the walls are known to be responsible for a highly fluctuating axial force on the penetrating object [127-129]. Even in gels, the long range of elastic deformations induced by the penetrating object will involve the wall properties of the container, such that the effective rigidity and toughness of the gel at the object scale will be modified depending on its distance to the wall. In real soils, the mobility of soil particles decreases spatially with depth [25] or with the proximity from an embedded wall or rigid obstacle, but also temporally as the seasonal drying changes the cohesion between particles hence the typical particle size that has to be displaced by the root progression.

2.3. Reorientation of root growth direction

Roots are flexible organs that follow tortuous paths in the soil. Roots skirt around obstacles on their trajectory through reorientation and continue their growth in the soil, apparently seeking out the path of least mechanical resistance. This statement, often found in the literature, should not be interpreted as a finalistic vision of root reorientation. Indeed, root path depends on the local mechanical stresses experienced by the root apex and some analogies might be drawn with the patterns of crack propagation during hydraulic fracturing in rigid pastes or of viscous fingering during the penetration of a high-viscosity fluid by a lower viscosity fluid [130]. Major change in root trajectory might also be beneficial for the root anchorage as was noted by Bengough *et al.* [6]. Then the reaction force due to the pushing exerted by the growing zone will be partly transferred to the soil at the bend of the root.

The exploration capability of roots is related to phenomena like circumnutation, buckling, thigmotropism or gravitropism but the interplay between them is difficult to decipher. In the following, we tempt to decompose the mechanisms involved in the reorientation of the root apex. Phototropism, hydrotropism or thermotropism, i.e. root growth reorientation due to light, humidity or temperature gradients are out of the scope of this review.

a) Reorientation of root growth direction through lasting contact with an obstacle: buckling and/or differential growth?

In this part, we focus on the reorientation of the root axis following the contact of the root tip with a permanent obstacle that blocks the initially straight root trajectory. In soils, this happens when the root apex has to cope with rigid obstacles like stones, hardpans or soil layers of larger strength (**Fig. 2A**). In structured soils, when a root grows across a macro-pore and meets a solid surface (**Fig. 2B**), it is unconfined laterally and may buckle, which reorients its growth direction (see the review by Jin *et al.* [7]).

Reorientations of the root growth direction have been investigated in different model experiments by putting a stiff obstacle perpendicular to the root axis, either a rigid obstacle [20, 131], or a stiff agar gel [132-134] or even a cantilever beam with a given flexibility [64]. Reorientation of the growth direction manifests itself through root bending. The origin of the bending can be passive through the buckling phenomenon (**Fig. 8**) or active through differential growth across the root section. In both cases, the induced curvature dissymetrises the root axis, then cells on the convex side are stretched while cells on the concave side are compressed. These differential strains can trigger internal signals

and induce an active response even in the case where the bending was initially provoked by buckling. The timescale of the curvature setting and its location relative to root zones help in distinguishing between passive or active phenomena.

In the model experiment of roots growing inside gels, Massa *et al.* [131] inserted a horizontal glass barrier acting as a permanent and rigid obstacle to the root growth of some species like *Arabidopsis*, *Phleum* and *Lepidium*. They observed a rapid bending of the root followed by a slippage of the root tip sideways. This bending occurred during the first 10 min after contact between the root apex and the glass barrier and the corresponding curvature was detectable in a zone that they attributed to the elongation zone. Due to the small timescale involved, the initiation of this bending might alternatively be interpreted as buckling. This first bending should not be mixed up with a second one that appears later on and which is located closer to the apex (see further at the end of part 2.3.b).

Buckling can be observed even if the obstacle is not infinitely rigid (**Fig. 9**). In the experiment of Bizet *et al.* [64], the obstacle was a force sensor made of a fine glass blade (**Fig. 9B**). Roots were grown in hydroponics either freely or in a laterally open needle that braces them without affecting their growth rate. The force applied by growing roots increased more than 15-fold when buckling was prevented by lateral bracing of the root. In the experiment of Silverberg *et al.* [132], roots of *Medicago truncatula* grown in hydrogels made of a compliant upper layer on top of a stiff lower layer buckled at the interface between the two gels before entering the lower gel. In this case where the root was fully embedded in the constraining upper gel of known stiffness, the modes of buckling differed from the classical Euler buckling described in **Fig. 8**. Contrary to the case of a root growing in a macro-pore where Euler buckling was expected with a long-wavelength post-buckling shape extending over the entire non-supported length (schematic diagram of **Fig. 8B** and hydroponics experiment of **Fig. 9B**), roots embedded in gels experienced a localized helical twist above the interface. The average vertical extent of the helix, as well as its averaged squared radius, were observed to scale like the inverse power law of the upper gel shear modulus G [132]. More precisely, the typical vertical length scale ℓ over which the root buckled was given by the following scaling law

$$\ell \sim \left(\frac{EI}{G} \right)^{1/4}$$

involving also the bending modulus EI of the root. This localized mechanism of buckling observed at the interface of gels of different rigidities in the experiments of Silverberg *et al.* [132] and also visible in **Fig. 9A**, might also occur at the interface between solid regions of different strengths in inhomogeneous soils. In this case, the buckling length scale depends on the elastic moduli of the surrounding constraining soil.

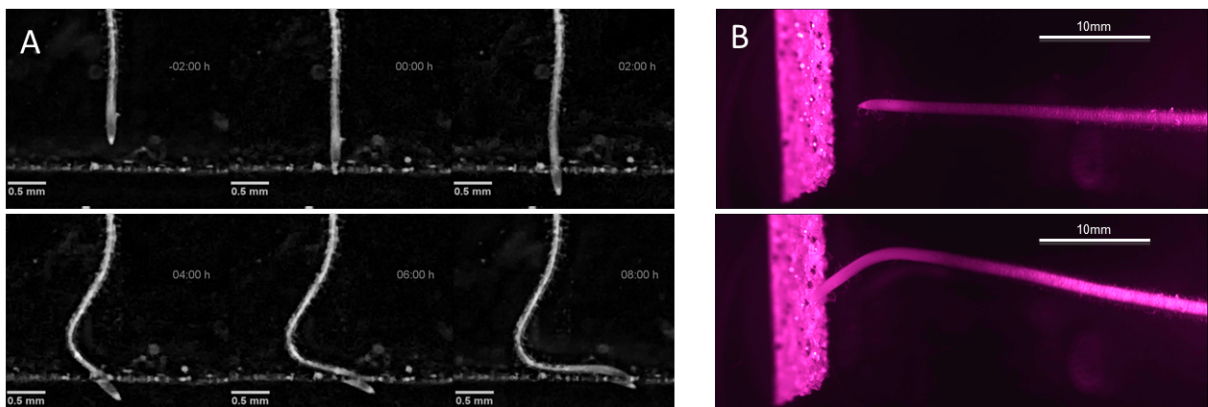


Fig. 9: Encounter of a root with obstacles. (A) Time course of a primary root of Arabidopsis thaliana growing initially vertically in a growth medium containing 0.2% of phytigel and encountering a harder medium containing 0.5% of phytigel (Images were taken every 2 hours). The root tip reorientation is clearly visible within 4 h of contact and might be interpreted as a buckling effect. After that, the root grows along the medium interface and tends to reorient towards the gravity direction (Courtesy of J. Roué). (B) Images of a poplar root growing horizontally against a glass blade in hydroponics, before (top) and after (bottom) buckling (Courtesy of F. Bizet).

Thus the root lateral confining medium must be taken into account, since it plays a role both in the buckling force threshold and in the way the root is deflected (post-buckling shape). Model experiments with mechanical root-analogous rod devices are needed to better understand the bending and post-buckling of embedded elongated objects in confining medium, whatever they are, gels [135], frictional tube [136, 137], or even granular media [138, 139].

The root growth against an obstacle creates a progressively increasing compression force in the root. If this compression force reaches a critical value while the root tip is still in contact with the obstacle, buckling can occur. When the root extremity is not supported laterally (like the schematics drawing in **Fig. 8** or the root growth in hydroponics of **Fig. 9B**), the buckling threshold is given by Euler formula. According to this formula (7) described in part 2.2, estimation of the buckling threshold requires a good determination of the root diameter d and also of the Young modulus E of the root tissue. The values for E reported in the literature span extremely broad range, especially for non-lignified tissues, ranging from a few to hundreds of MPa [64]. The elastic moduli of plant tissues are known to change with time, stress, physiological status and the dimensions of the tissue samples. The values also differ amongst root types, ages or locations in the apex [140-142]. Most of these rigidity measurements were done on excised fragments of root that can severely dry during the mechanical tests. Yet changes in water content that lead to changes in cell turgor pressure modifies the tension in the cell wall, which impacts the macroscopic mechanical properties like the tissue elastic modulus. Moreover, root is a complex multicellular tissue with mechanical anisotropy: its mechanical response differs according to the direction and mode of loading (compression, traction, flexion or oscillatory loadings). Depending on the amplitude or rate of deformation during loading, the root might not follow a linear elastic behavior [143] but rather a visco-elastic behavior with poro-elastic processes (water transport through the cell walls induced by the loading) [144]. Therefore the determination of the Young modulus of a root tissue is not straightforward and the protocol should be carefully specified if we want to use a correct value of E for estimating a buckling threshold for growing roots.

According to the work of Dexter and Hewitt [117], the mechanisms of root penetration in a structured impeding soil will depend on the relative value of the soil strength to the buckling stress of the root when growing in a macro-pore. The soil strength can be measured by a penetrometer and the corresponding normal stress σ_{soil} exerted by the soil that opposes root growth at its tip can be inferred by supposing that roots experience a stress 2 to 8 times smaller than the penetrometer. But roots cannot exert a growth pressure larger than σ_{Max} . Thus when the soil has a large strength and is hardly deformable ($\sigma_{soil} > \sigma_{Max}$), we have to compare the maximal stress σ_{Max} (defined in part 2.1.a) to the buckling stress $\sigma_B = \frac{F_B}{S}$, where $S = \frac{\pi d^2}{4}$ is the root cross-section. In the case depicted in **Fig. 8** of a root growing inside a macro-pore (that is an air gap where the root extremity is not supported laterally over a length ℓ), we use the classical Euler formula (7) for the buckling force. Thus we have to compare σ_{Max} to

$$\sigma_B \sim \frac{Ed^4}{\ell^2 d^2} = E \left(\frac{d}{\ell} \right)^2$$

If $\sigma_B < \sigma_{Max}$, the root will buckle before stopping its axial growth [117]. For an initially straight penetration, buckling will consequently lead to a change in the orientation of the root apex with regards to the initial growth direction. Thus a root has the possibility to skirt around a too rigid obstacle or soil layer. In the case where the initial root growth axis is along the gravity, buckling will reorient the root apex relative to the gravity direction, thus competing with gravitropic response.

In the opposite case, if $\sigma_{Max} < \sigma_B$, the root will stop its growth before buckling can occur, unless the circumnutation movements and/or thigmotropic responses (see part 2.3.b) reorient growth direction before the maximum growth pressure σ_{Max} is reached.

Alternatively the comparison between σ_{Max} and σ_B gives a critical length ℓ_C for the transition between the two preceding cases [145]. For structured soils, the length ℓ is the distance over which the root is not supported laterally when growing inside a fixed macro-pore. Thus $\sigma_{Max} = \sigma_B$ provides an interesting scaling for the critical length of the pore size, that we write in the following way:

$\ell_C \sim \sqrt{\frac{E}{\sigma_{Max}}} d$. When the pore size is below ℓ_C and for hardly deformable soil ($\sigma_{Soil} > \sigma_{Max}$) straight penetration will be limited by the maximum growth pressure σ_{Max} and not by buckling. According to equation (4), an estimation of σ_{Max} is provided by $\sigma_{Max} \sim P$, where P is the turgor pressure. Thus ℓ_C can be rewritten as $\ell_C \sim \sqrt{\frac{E}{P}} d$. A reasonable value of Young modulus E , ten to hundred times larger than the turgor pressure P , gives $\ell_C \sim 3d$ to $10d$, so $\ell_C \sim 3 - 10$ mm for a millimeter root diameter d . This has to be compared with the typical air gaps in the soils, which are often in the range between 0 and 3 mm [145].

In all the preceding cases, the stiffness of the impeding obstacle at the root tip has been supposed to be large enough compared with the root's stiffness. Indeed in the case where the stiffness of the obstacle (force sensor, soil layer or wall) has a finite value, the root grows and pushes the obstacle ahead. This will change the slope of the evolution of the compression force with time but a priori not the Euler buckling scaling for a non-fully embedded root growing against this stiff obstacle. Therefore changing the stiffness of the force sensor in model experiments is of particular interest for changing the timescale of loading compared to the typical timescale(s) of biological regulation of the root in response to obstacle.

In the case of a continuous soil with no macro-pore, the root might still buckle at the interface between regions of different strengths. The modes of buckling differ and also depend on the radial and tangential components of the stress field applied by the confining soil at the root periphery, as it was observed in the model experiments of rods or roots embedded in constraining gel media.

b) Role of circumnutation in obstacle avoidance?

The growing tip of most rapidly elongating plant organs exhibits some intriguing bending movements in different directions around the main growth direction (see the review of Rivière *et al.* [146]). As early as 1880, Charles and Francis Darwin in their book '*The power of movement of plants*' introduced the term *circumnutation* to describe these movements [5]. Circumnutation is now generally defined as helical movement of growing organs which vary in amplitude and frequencies [147-149]. These rhythmic oscillations are outlined by the organ tip movement whose planar projection describes circular, elliptical, pendulum-like or irregular zig-zag tracks with periods of the order of several

minutes to several hours superimposed on circadian and infradian rhythms [150]. These movements exist in roots whatever the orientation of their main trajectory, along the gravity (tap root) or along a tilted direction (laterals). They occur even in the absence of any anisotropic mechanical stress, as they were also clearly observed for root growth in aeroponics, hydroponics or in homogeneous gels.

Well described in stem parts, information regarding the root tip motion is limited and the detailed physiological mechanisms underlying these movements are largely unknown, leading to controversial hypotheses [149]. Using time-lapse photography, Kim *et al.* [151] monitored in detail the root tip movements of *Pisum sativum* seedling and showed that the rhythmic oscillations were continual during the one day duration of the study and circular, with a period of approximately 2.5 hours. Seminal roots of young rice seedlings displayed circumnutation with a 4.7 hours helix period [152]. The rhythmicity depends on plant species and one hypothesis is that it is endogenously regulated and driven by an internal oscillator. In stem, the internal oscillator was suspected to be a differential growth wave travelling along the elongating organ [153, 154]. These growth waves could be coupled with the oscillation of growth substances such as auxin [151].

Some studies have shown that the regularity of circumnutation pattern can be affected by external signals such as the wavelength of light [152], the temperature or the composition of the growth medium [155, 156]. Thus circumnutation is not solely explained by endogenously regulated mechanisms [157]. When circumnutating, the growing root tip is submitted to continuous changes of the orientation of its gravisensory apparatus (the statolites) relative to the gravity and gravitropic responses might also be involved in the root movements. This is supported by several experiments, where impaired circumnutation is observed for agravitropic mutants (i.e. unable to sense gravity) [151, 158]. Similarly, the removal of the root cap (site of gravity sensing in roots) from pea roots attenuated the gravitropic response and had an effect on root circumnutation [151]. Amplitude, period, shape and direction of circumnutating movements can also be affected by direct mechanical stress or stimulus like rubbing or touching. In many studies, seedlings grow on the surface of semi-solid media (such as agar or phytigel) in Petri dishes [155, 156], such that the roots are in contact with the medium on one side and exposed to air on the other side. The root tip might experience some friction with the gel surface [159], that could be perceived by the root as a physical constraint and could induce a response to contact, called thigmotropism. Some studies clearly showed that roots of seedlings grown on inclined agarose gels exhibited both deviation from the steepest slope trajectory, known as skewing movements, and root waving with sinusoidal growth pattern [133, 148, 159]. Thus, the root tip deviations from the main growth axis are complex to describe and might arise from both endogenously regulated mechanisms and growth responses to external signals such as gravity or mechanical contact.

One important point to consider is the impact of these root tip movements in the soil. It is conceivable that these movements are integrated in the process of soil penetration and thus have an ecological significance. Circumnutation has been observed to play a role in the penetration of continuous soils. Comparing seedlings of various rice varieties, Inoue *et al.* [160] showed that root tips experiencing large spiral angles from the main growth direction were more efficient to penetrate flooded or very soft soils. In structured soils, circumnutation is sometimes viewed as a way for roots to explore the lateral environment and find pathways of less mechanical resistance like cracks and biopores, but the detailed mechanisms of “soil exploration” are unclear. Circumnutation may change the angle of incidence at which a root meets an interface of different strength in the soil. Indeed the proportion of roots penetrating a medium of large strength after having grown in a weak strength medium is not only a function of the mechanical properties of root and media, but also of the angle of incidence. In the work of Dexter *et al.* [117], roots growing vertically in a small air gap contacted a second medium

whose planar interface was inclined at different angles. The roots arriving with a more oblique incidence (due in this case to the inclination of the interface) had a lower probability to enter the second medium and were deflected sideways along the planar interface. The same effect should occur if circumnutation deflects the root apex from a normal incidence just before the root cap contacts the interface. Following the contact, mechanical stress will be exerted asymmetrically on the root cap and some thigmotropic response can occur, the root tip bending towards the direction opposite to contact. This mechanism might occur for a gravitropic root growing mainly vertically but experiencing circumnutation and encountering a horizontal strong layer in a soil with an oblique incidence. This might be a first step toward a reorientation of the growth axis and the possibility of lateral exploration for the root. Thus circumnutation and thigmotropism, like buckling, might help roots to skirt around obstacles.

Whatever the origins of the root growth reorientation and associated bending of the root axis following the contact with a stronger interface, it is often observed that the root tip also reorients later to point downwards [131] (**Fig. 9A**, Roué and Legué, unpublished results). This second curvature closer to the apex is interpreted as a gravitropic response and may help the root to resume its downward growth as soon as the interface ends.

c) Impact of changes of growth direction on the root system architecture

Besides reorienting the growth direction, another possible consequence of the root bending is the formation of laterals. For instance, in the experiments of Ditengou *et al.* [161] or Richter *et al.* [162], a root curvature has been induced externally by manual bending or internally by reorientation of growth direction consecutive to buckling or gravitropism. As a consequence, lateral roots are formed from the pericycle cells and are observed to emerge on the convex side of the bent root. These laterals generate a different root architecture pattern.

d) Mechanoperception and signalling pathways

The mechanism of obstacle perception has not been clearly demonstrated. The cells of the root cap are the firsts to encounter obstacles through the soil, making them strong candidates to sense soil strength. These cap cells have long been proposed as a site of sensing, including gravity (gravitropism) and contact sensing (thigmotropism). The sensitiveness of the root cap to contact was already mentioned in Darwin's work. Affixing a small piece of a visiting card, very thin glass or sand paper on one side of the conical part of a bean root apex caused the radicle to bend within a few hours to the other side [5]. In this kind of experiments, as soon as the root bends, its inclination changes, inducing a gravitropic stimulus and leading to the re-orientation of root growth toward the vertical position [131]. This leads to combined thigmo- and gravi-tropic responses for the root growth, difficult to disentangle [163]. Other experiments measuring the forces exerted by the root apex suggest that the root cap cells could sense contact. In the work of Bizet *et al.* [64], a horizontal growing poplar root encounters an obstacle acting as a force sensor (a beam cantilever), such that root growth rate and force applied by the root could be simultaneously monitored (**Fig. 9B**). The root growth was strongly reduced or stopped for a ten of minutes just after the contact of the root cap against the force sensor and before any significant resisting force built up (<0.2 mN), supporting the idea that the root cap could be one sensing site. This

hypothesis is also supported by our recent experiments with *Arabidopsis* mutants, in which the formation of the root cap is affected. Their root growth response to harder phytagel medium differs from the one of the wild type (**Fig. 9A**, Roué and Legué, unpublished results).

How mechanical constraints are sensed in plants, how the cells sense their local mechanical state and how they induce responses are long-standing questions. In contrast with gravisensing for which the perception zone has been located in the columella cells of the root cap, for thigmosensing there seems to be no specific mechano-perceptive tissue. Biomechanical models are helpful tools to define quantitative behaviors and to identify the variable(s) that is (are) sensed (review of Moulia *et al.* [164]). For instance, it was shown that the bending of tomato stem base induces a temporary inhibition of the stem elongation. Though, the stem elongation zone is far away from the bending site, indicating that the response zone can be at a long distance from the perception zone of the mechanical stimuli [163]. Based on controlled bending experiments, Coutand *et al.* [165] showed that the mechanosensing and responses depend on the load, the mechanical structure of the organ and the mechanosensitive structure, that is the location and amount of mechanosensitive tissues involved in the response. They demonstrated that the variable which is perceived is the strain and that the duration of the plant response is correlated to the spatial sum of longitudinal strains in the bent part. They proposed an integrative model of mechanosensing, in which the sum of strains is perceived and triggers signalisation and growth response.

At the cell scale, the stress perception likely occurs through sensing the deformation of the cell wall and appressed plasma membrane via the activation of mechanosensors [166]. Mechanosensitive ion channels (MS), a specialized class of ion channels which respond to mechanical load in the membrane are considered as the main mechano-receptors [167, 168]. Ion channels are membrane-embedded protein complexes that provide a pathway for ions through the membrane lipid bilayer. Molecular mechanisms involved in mechano-perception have been particularly well studied in bacterial and animal systems. In plants, two simplified models have been proposed in the literature: MS ion channels open directly by an increase of membrane tension or indirectly by the pulling of tethers connected to the cytoskeleton or the cell wall [168].

An important piece of work has focused on the identification and characterisation of diverse mechanosensors (reviews of [20, 168-170]). Among them, MCA1, a member of the MCA family, is particularly well characterised [171-173]. MCA1 is a plasma membrane protein, that was identified as a mechano-stimulated Ca^{2+} channel, i.e. a channel which opens in response to mechanical stresses and let Ca^{2+} ions to permeate [172]. Using the two-layers-agar method, [171] showed that unlike wild-type, the primary roots of a significant proportion of the *mca1*-null seedlings (mutants not expressing MCA1) were unable to penetrate in a hard agar layer after having grown through an upper soft agar medium. Therefore, the authors suggest that MCA1 is required for sensing the hardness of agar or soil and is crucial for the mechanosensing in the primary root. Interestingly, the studies of MCA1 expression reveal that the corresponding mechano-sensor is located in the meristem and elongation zone of *Arabidopsis* primary roots, but not in the root cap [134], suggesting the site of mechanosensing is not restricted to the root cap.

The signalling cascade, i.e. the series of cellular events leading to the physiological response, follows the sensing of the mechanical stress. Recent studies with molecular and genetic approaches as well as imaging techniques have begun to decipher the signalling pathways in roots, from the sensing to the response, including the transmitting information [174]. One of the first responses is an increase of intracellular calcium ion (Ca^{2+}) concentration. For example, mechanically perturbing a single root

epidermal cell by touching it with a glass micropipette elicits an increase in cytosolic Ca^{2+} at the site of touch within 1 to 18 s after initiation of the stimulus [166, 175]. A Ca^{2+} signature is observed in response to different types of mechanical stimuli, such as local touch or bending through an external force or indirectly by encountering an obstacle. All these observations suggest that Ca^{2+} signal is an early and intrinsic response to mechanical stress. Mechanical stresses also trigger rapid production of ROS (reactive oxygen species) in the cell wall and proton influx to the cytoplasm, with concomitant cell wall alkalisation, leading to transient changes in pH [166]. These biochemical changes in cell wall environment might cause the cell wall mechanical properties to vary accordingly. As a consequence, the cell wall extensibilities and yield stress are modified, which in turn affects the whole process of cell growth.

Clearly the identification of mechanosensors and signalling pathways are intense research areas and the detailed cascade of events from the perception of mechanical stresses till the change in root growth are still unknown.

Conclusions

In this review we have discussed the main elementary mechanisms involved in the root penetration of soils: i) axial thrust produced by a turgor driven anisotropic cell growth, ii) radial swelling reducing the axial resistance of the soil in front of the root tip or stabilizing the root axis against buckling, and iii) reorientation of the root apex by passive and active mechanisms like root buckling or differential growth across the root section.

Understanding the root growth pattern from the individual physical interaction of the root apex with obstacles or soil patches of large resistance is a great challenge for modeling and poses a number of fundamental questions regarding sensing, transduction and adaptive response to mechanical stress. Imagining that these questions could be solved opens the possibility of “root engineering”: By placing obstacles of different stiffness and shapes at different soil depths, one could imagine reorienting the root path and inducing the branching pattern [161, 162]. Controlling the phenotypic plasticity of roots is the ultimate goal for designing the most efficient root architecture for a given purpose. In crop science and agriculture, optimizing the root architecture is of particular interest for insuring good plant anchorage against overturning or lodging and for improving water and nutrient uptake according to their spatial availability in soil. In civil engineering and soil science, it is also important to design the optimal root architecture for stabilizing slopes against landslides and soil erosion.

Plant root strategies of soil exploration have recently inspired other domains in bio-mimetism and soft robotics. Due to their growth process wherein new cells are added at the root apex while mature cells remain stationary relative to the soil, plant roots offer a good example of digging efficiency by insuring a good anchorage and by minimizing lateral friction. Based on this mechanism of tip growth, Sadeghi *et al.* [176] have designed a digging robot, in which some new material is continuously added layer by layer at the tip area while the rest of the tubular device stays stationary. The performance of this robot was better in terms of energy consumption and penetration speed compared with the same device simply pushed from the top into the soil. In soft robotics, there is a need for device capable of soft movements to reach precision and sensitivity. In the ‘Plantoid’ robot [177], the bending capabilities of roots are reproduced through differential elongation of soft spring-based actuators. In addition, these soft movements are activated in response to sensors located at the tip to mimic the supposed ability of the root apex to detect gravity, temperature, humidity and touch stimuli. In

particular, the thigmotropism of roots is reproduced, as the robotic root bends in order to avoid obstacles.

Another emerging application field comes from microfluidics for investigating plants and especially plant roots. In the ‘Rootchip’ project [178], microfluidic chip platforms were designed for good control and rapid modulation of environmental conditions as well as for live-cell imaging of *Arabidopsis thaliana* roots cultured in parallel. Certainly, microfluidic devices [179] open up new avenues for investigating physical root-soil interaction.

Acknowledgments

The authors are grateful to Arezki Boudaoud (ENS Lyon, France) and the editorial board for the invitation to contribute to this special issue. This work was supported by the French National Research Agency through the Laboratory of Excellence ARBRE (ANR-12- LABXARBRE-01) for M.B.B.T. and by the French Space Agency (CNES) and ANR Blanc Grap2 (ANR-13- BSV5-0005-01) for V.L. E.K. is particularly grateful to all the members of the ROSOM project through the program of Agropolis Foundation (reference ID 1202-073) (Labex Agro: ANR-10-LABX-001-01). We particularly thank Alain Pierret (IRD, Lao) for its support and advice and for reading some parts of the manuscript. We also kindly thank Laurette S. Tuckerman (PMMH, ESPCI, France) for the English corrections.

References

- [1] Walter A, Silk W K and Schurr U 2009 Environmental effects on spatial and temporal patterns of leaf and root growth *Annual Review of Plant Biology* **60** 279-304
- [2] Pierret A, Hartmann C, Maeght J L and Pagès L 2011 *The Architecture and Biology of Soils: Life in Inner Space*, pp 86-103
- [3] Rellán-Álvarez R, Lobet G and Dinneny J R 2016 Environmental Control of Root System Biology. In: *Annual Review of Plant Biology*, pp 619-42
- [4] Babe A, Lavigne T, Severin J P, Nagel K A, Walter A, Chaumont F, Batoko H, Beeckman T and Draye X 2012 Repression of early lateral root initiation events by transient water deficit in barley and maize *Philosophical Transactions of the Royal Society of London. Series B, Biological Sciences* **367** 1534-41
- [5] Darwin C and Darwin F 1880 *The power of movement in plants* (London: John Murray)
- [6] Bengough A G, McKenzie B M, Hallett P D and Valentine T A 2011 Root elongation, water stress, and mechanical impedance: a review of limiting stresses and beneficial root tip traits *J. Exp. Bot.* **62** 59-68
- [7] Jin K, Shen J, Ashton R W, Dodd I C, Parry M A J and Whalley W R 2013 How do roots elongate in a structured soil? *J. Exp. Bot.* **64** 4761-77
- [8] Tracy S R, Black C R, Roberts J A and Mooney S J 2011 Soil compaction: a review of past and present techniques for investigating effects on root growth *Journal of the Science of Food and Agriculture* **91** 1528-37
- [9] Gregory P J, Bengough A G, Grinev D, Schmidt S, Thomas W T B, Wojciechowski T and Young I M 2009 Root phenomics of crops: opportunities and challenges *Functional Plant Biology* **36** 922-9
- [10] Passioura J B 2002 'Soil conditions and plant growth' *Plant Cell and Environment* **25** 311-8
- [11] Pagès L 2016 Branching patterns of root systems: Comparison of monocotyledonous and dicotyledonous species *Annals of Botany* **118** 1337-46
- [12] Silk W K 1992 Steady form from changing cells *International Journal of Plant Sciences* **153** S49-S58
- [13] Erickson R O and Sax K B 1956 Elemental growth rate of the primary root of ze mays *Proceedings of the American Philosophical Society* **100** 487-98
- [14] Richards W and Kavanagh A J 1943 The analysis of the relative growth gradients and changing form of growing organisms: illustrated by the tobacco leaf *American Naturalist* **77** 385-99
- [15] Arnaud C, Bonnot C, Desnos T and Nussaume L 2010 The root cap at the forefront *C R Biol* **333** 335-43
- [16] Kumpf R P and Nowack M K 2015 The root cap: a short story of life and death *J. Exp. Bot.* **66** 5651-62
- [17] Driouich A, Durand C and Vitré-Gibouin M 2007 Formation and separation of root border cells *Trends in Plant Science* **12** 14-9
- [18] Schenk H J 2008 Soil depth, plant rooting strategies and species' niches *New Phytologist* **178** 223-5
- [19] Bengough A G 2003 *Root Ecology*, ed H de Kroon and E J Visser (Berlin, Heidelberg: Springer Berlin Heidelberg) pp 151-71
- [20] Monshausen G B and Gilroy S 2009 The exploring root — root growth responses to local environmental conditions *Current Opinion in Plant Biology* **12** 766-72
- [21] Dexter A R 1988 Advances in characterization of soil structure *Soil & Tillage Research* **11** 199-238
- [22] U.S. S C S 1993 Soil Survey Division Staff. Soil survey manual. Department of Agriculture Handbook 18

- [23] Meysman F J R, Middelburg J J and Heip C H R 2006 Bioturbation: a fresh look at Darwin's last idea *Trends in Ecology & Evolution* **21** 688-95
- [24] Ghezzehei T A and Or D 2000 Dynamics of soil aggregate coalescence governed by capillary and rheological processes *Water Resources Research* **36** 367-79
- [25] Whiteley G M and Dexter A R 1984 Displacement of soil aggregates by elongating roots and emerging shoots of crop plants *Plant Soil* **77** 131-40
- [26] Vollsnes A V, Futsaether C M and Bengough A G 2010 Quantifying rhizosphere particle movement around mutant maize roots using time-lapse imaging and particle image velocimetry *European Journal of Soil Science* **61** 926-39
- [27] Kolb E, Hartmann C and Genet P 2012 Radial force development during root growth measured by photoelasticity *Plant Soil* **360** 19-35
- [28] Fakihi M, Delenne J Y, Radjai F and Fourcaud T 2016 Contribution of mechanical factors to the variability of root architecture: Quantifying the past history of interaction forces between growing roots and soil grains. In: *Proceedings - 2016 IEEE International Conference on Functional-Structural Plant Growth Modeling, Simulation, Visualization and Applications, FSPMA 2016*, pp 52-60
- [29] Faure A G 1994 Stress Field Developed by Root Growth: Theoretical Approach *J. Agr. Eng. Res.* **58** 53-67
- [30] Kirby J M and Bengough A G 2002 Influence of soil strength on root growth: experiments and analysis using a critical-state model *European Journal of Soil Science* **53** 119-27
- [31] McKenzie B M, Mullins C E, Tisdall J M and Bengough A G 2013 Root-soil friction: quantification provides evidence for measurable benefits for manipulation of root-tip traits *Plant Cell and Environment* **36** 1085-92
- [32] Bengough A G and Mullins C E 1990 Mechanical impedance to root-growth - a review of experimental-techniques and root-growth responses *Journal of Soil Science* **41** 341-58
- [33] van Noordwijk M, Brouwer G and Harmanny K 1993 Concepts and methods for studying interactions of roots and soil structure *Geoderma* **56** 351-75
- [34] Batey T 2009 Soil compaction and soil management - A review *Soil Use and Management* **25** 335-45
- [35] Niklas K J 1992 *Plant Biomechanics: An Engineering Approach to Plant Form and Function*: University of Chicago Press Books)
- [36] Richefeu V, El Youssoufi M S and Radjai F 2006 Shear strength properties of wet granular materials *Physical Review E - Statistical, Nonlinear, and Soft Matter Physics* **73** 051304
- [37] Kramer P J and Boyer J S 1995 *Water relations of plants and soils* (San Diego: Academic Press)
- [38] Whitmore A P and Whalley W R 2009 Physical effects of soil drying on roots and crop growth *J. Exp. Bot.* **60** 2845-57
- [39] Atwell B J 1990 The effect of soil compaction on wheat during early tillering.1 *New Phytologist* **115** 29-35
- [40] Whiteley G M and Dexter A R 1982 Root development and growth of oilseed, wheat and pea crops on tilled and non-tilled soil *Soil & Tillage Research* **2** 379-93
- [41] Mirreh H F and Ketcheson J W 1973 Influence of soil-water matric potential and resistance to penetration on corn root elongation *Canadian Journal of Soil Science* **53** 383-8
- [42] Taylor H M and Ratliff L F 1969 Root elongation rates of cotton and peanuts as a function of soil strength and soil water content *Soil Science* **108** 113-&
- [43] Barley K P 1962 Effects of mechanical stress on growth of roots *J. Exp. Bot.* **13** 95
- [44] Iijima M and Kato J 2007 Combined soil physical stress of soil drying, anaerobiosis and mechanical impedance to seedling root growth of four crop species *Plant Production Science* **10** 451-9
- [45] Veen B W and Boone F R 1990 The influence of mechanical resistance and soil-water on the growth of seminal roots of maize *Soil & Tillage Research* **16** 219-26

- [46] Croser C, Bengough A G and Pritchard J 1999 The effect of mechanical impedance on root growth in pea (*Pisum sativum*). I. Rates of cell flux, mitosis, and strain during recovery *Physiol. Plant.* **107** 277-86
- [47] Loades K W, Bengough A G, Bransby M F and Hallett P D 2013 Biomechanics of nodal, seminal and lateral roots of barley: effects of diameter, waterlogging and mechanical impedance *Plant Soil* **370** 407-18
- [48] Bengough A G and Young I M 1993 Root elongation of seedling peas through layered soil of different penetration resistances *Plant Soil* **149** 129-39
- [49] Clark L J, Whalley W R and Barraclough P B 2003 How do roots penetrate strong soil? *Plant Soil* **255** 93-104
- [50] Goss M J and Russell R S 1980 Effects of mechanical impedance on root-growth in barley (*hordeum-vulgare*-l) .3. Observations on the mechanism of response *J. Exp. Bot.* **31** 577-88
- [51] Atwell B J 1988 Physiological-responses of lupin roots to soil compaction *Plant Soil* **111** 277-81
- [52] Materechera S A, Dexter A R and Alston A M 1991 Penetration of very strong soils by seedling roots of different plant-species *Plant Soil* **135** 31-41
- [53] Materechera S A, Alston A M, Kirby J M and Dexter A R 1992 Influence of root diameter on the penetration of seminal roots into a compacted subsoil *Plant Soil* **144** 297-303
- [54] Misra R K and Gibbons A K 1996 Growth and morphology of eucalypt seedling-roots, in relation to soil strength arising from compaction *Plant Soil* **182** 1-11
- [55] Bingham I J and Bengough A G 2003 Morphological plasticity of wheat and barley roots in response to spatial variation in soil strength *Plant Soil* **250** 273-82
- [56] Thaler P and Pages L 1999 Why are laterals less affected than main axes by homogeneous unfavourable physical conditions? A model-based hypothesis *Plant Soil* **217** 151-7
- [57] Goss M J 1977 Effects of mechanical impedance on root-growth in barley (*hordeum-vulgare*-l) .1. Effects on elongation and branching of seminal root axes *J. Exp. Bot.* **28** 96-111
- [58] Vocanson A, Roger-Estrade J, Boizard H and Jeuffroy M H 2006 Effects of soil structure on pea (*Pisum sativum* L.) root development according to sowing date and cultivar *Plant Soil* **281** 121-35
- [59] Clark L J, Whalley W R, Dexter A R, Barraclough P B and Leigh R A 1996 Complete mechanical impedance increases the turgor of cells in the apex of pea roots *Plant Cell and Environment* **19** 1099-102
- [60] Pfeffer W 1893 *Druck- und Arbeitsleistung durch wachsende Pflanzen* (Leipzig: Hirzel, S.)
- [61] Gill W R and Bolt G H 1955 Pfeffer's studies of the root growth pressures exerted by plants *Agron Jour* **47** 166-8
- [62] Souty N 1987 Mechanical-behavior of growing roots .1. Measurement of penetration force *Agronomie* **7** 623-30
- [63] Clark L J, Bengough A G, Whalley W R, Dexter A R and Barraclough P B 1999 Maximum axial root growth pressure in pea seedlings: effects of measurement techniques and cultivars *Plant Soil* **209** 101-9
- [64] Bizet F, Bengough A G, Hummel I, Bogeat-Triboulot M B and Dupuy L X 2016 3D deformation field in growing plant roots reveals both mechanical and biological responses to axial mechanical forces *J. Exp. Bot.* **67** 5605-14
- [65] Misra R K, Dexter A R and Alston A M 1986 Maximum axial and radial growth pressures of plant roots *Plant Soil* **95** 315-26
- [66] Whalley W R and Dexter A R 1993 The maximum axial growth pressure of roots of spring and autumn cultivars of lupin *Plant Soil* **157** 313-8
- [67] Souty N and Stepniewski W 1988 The influence of external oxygen concentration on axial root-growth force of maize radicles *Agronomie* **8** 295-300
- [68] Azam G, Grant C D, Misra R K, Murray R S and Nuberg I K 2013 Growth of tree roots in hostile soil: A comparison of root growth pressures of tree seedlings with peas *Plant Soil* **368** 569-80

- [69] Misra R K 1997 Maximum axial growth pressures of the lateral roots of pea and eucalypt *Plant Soil* **188** 161-70
- [70] Clark L J and Barraclough P B 1999 Do dicotyledons generate greater maximum axial root growth pressures than monocotyledons? *J. Exp. Bot.* **50** 1263-6
- [71] Baskin T I 2013 Patterns of root growth acclimation: constant processes, changing boundaries *Wiley Interdisciplinary Reviews-Developmental Biology* **2** 65-73
- [72] Lockhart J A 1965 An Analysis of Irreversible Plant Cell Elongation *Journal of Theoretical Biology* **8** 264-75
- [73] Geitmann A and Ortega J K E 2009 Mechanics and modeling of plant cell growth *Trends in Plant Science* **14** 467-78
- [74] Pritchard J 1994 The control of cell expansion in roots *New Phytologist* **127** 3-26
- [75] Crowell E F, Timpano H, Desprez T, Franssen-Verheijen T, Emons A M, Hofte H and Vernhettes S 2011 Differential Regulation of Cellulose Orientation at the Inner and Outer Face of Epidermal Cells in the Arabidopsis Hypocotyl *Plant Cell* **23** 2592-605
- [76] Dyson R J, Vizcay-Barrena G, Band L R, Fernandes A N, French A P, Fozard J A, Hodgman T C, Kenobi K, Pridmore T P, Stout M, Wells D M, Wilson M H, Bennett M J and Jensen O E 2014 Mechanical modelling quantifies the functional importance of outer tissue layers during root elongation and bending *New Phytologist* **202** 1212-22
- [77] Mirabet V, Das P, Boudaoud A and Hamant O 2011 *Annual Review of Plant Biology, Vol 62*, ed S S Merchant, *et al.* pp 365-85
- [78] Baskin T I 2005 Anisotropic expansion of the plant cell wall *Annual Review of Cell and Developmental Biology* **21** 203-22
- [79] Hamant O and Traas J 2010 The mechanics behind plant development *New Phytologist* **185** 369-85
- [80] Green P B 1964 Cell walls and the geometry of plant growth *Brookhaven Symposia in Biology* **16** 203-17
- [81] Wiedemeier A M D, Judy-March J E, Hocart C H, Wasteneys G O, Williamson R E and Baskin T I 2002 Mutant alleles of Arabidopsis RADIALLY SWOLLEN 4 and 7 reduce growth anisotropy without altering the transverse orientation of cortical microtubules or cellulose microfibrils *Development* **129** 4821-30
- [82] Baskin T I, Meekes H, Liang B M and Sharp R E 1999 Regulation of growth anisotropy in well-watered and water-stressed maize roots. II. Role of cortical microtubules and cellulose microfibrils *Plant Physiol.* **119** 681-92
- [83] Anderson C T, Carroll A, Akhmetova L and Somerville C 2010 Real-Time Imaging of Cellulose Reorientation during Cell Wall Expansion in Arabidopsis Roots *Plant Physiol.* **152** 787-96
- [84] Hamant O, Heisler M G, Jonsson H, Krupinski P, Uyttewaal M, Bokov P, Corson F, Sahlin P, Boudaoud A, Meyerowitz E M, Couder Y and Traas J 2008 Developmental Patterning by Mechanical Signals in Arabidopsis *Science* **322** 1650-5
- [85] Greacen E L and Oh J S 1972 Physics of root growth *Nature-New Biology* **235** 24-5
- [86] Bengough A G, Croser C and Pritchard J 1997 A biophysical analysis of root growth under mechanical stress *Plant Soil* **189** 155-64
- [87] Taiz L and Zeiger E 2006 *Plant Physiology*: Sinauer Associates, Inc.)
- [88] Boudaoud A 2010 An introduction to the mechanics of morphogenesis for plant biologists *Trends in Plant Science* **15** 353-60
- [89] Clark L J, Whalley W R and Barraclough P B 2001 Partial mechanical impedance can increase the turgor of seedling pea roots *J. Exp. Bot.* **52** 167-71
- [90] Atwell B J and Newsome J C 1990 Turgor pressure in mechanically impeded lupin roots *Australian Journal of Plant Physiology* **17** 49-56
- [91] Croser C, Bengough A G and Pritchard J 2000 The effect of mechanical impedance on root growth in pea (*Pisum sativum*). II. Cell expansion and wall rheology during recovery *Physiol. Plant.* **109** 150-9

- [92] Bengough A G and Mackenzie C J 1994 Simultaneous measurement of root force and elongation for seedling pea roots *J. Exp. Bot.* **45** 95-102
- [93] Frensch J and Hsiao T C 1994 Transient responses of cell turgor and growth of maize roots as affected by changes in water potential *Plant Physiol.* **104** 247-54
- [94] Silk W K and Bogeat-Triboulot M B 2014 Deposition rates in growing tissue: Implications for physiology, molecular biology, and response to environmental variation *Plant Soil* **374** 1-17
- [95] Merret R, Moulia B, Hummel I, Cohen D, Dreyer E and Bogeat-Triboulot M B 2010 Monitoring the regulation of gene expression in a growing organ using a fluid mechanics formalism. In: *BMC Biology*, p 18
- [96] Baluska F, Mancuso S, Volkmann D and Barlow P W 2010 Root apex transition zone: a signalling-response nexus in the root *Trends in Plant Science* **15** 402-8
- [97] Bizet F, Hummel I and Bogeat-Triboulot M B 2015 Length and activity of the root apical meristem revealed in vivo by infrared imaging *J. Exp. Bot.* **66** 1387-95
- [98] Bengough A G and McKenzie B M 1997 Sloughing of root cap cells decreases the frictional resistance to maize (*Zea mays* L.) root growth *J. Exp. Bot.* **48** 885-93
- [99] Iijima M, Higuchi T, Barlow P W and Bengough A G 2003 Root cap removal increases root penetration resistance in maize (*Zea mays* L.) *J. Exp. Bot.* **54** 2105-9
- [100] Hawes M C, Bengough G, Cassab G and Ponce G 2002 Root caps and rhizosphere *Journal of Plant Growth Regulation* **21** 352-67
- [101] Bais H P, Weir T L, Perry L G, Gilroy S and Vivanco J M 2006 *Annual Review of Plant Biology*, pp 233-66
- [102] Carminati A, Moradi A B, Vetterlein D, Vontobel P, Lehmann E, Weller U, Vogel H J and Oswald S E 2010 Dynamics of soil water content in the rhizosphere *Plant Soil* **332** 163-76
- [103] Read D B and Gregory P J 1997 Surface tension and viscosity of axenic maize and lupin root mucilages *New Phytologist* **137** 623-8
- [104] Read D B, Bengough A G, Gregory P J, Crawford J W, Robinson D, Scrimgeour C M, Young I M, Zhang K and Zhang X 2003 Plant roots release phospholipid surfactants that modify the physical and chemical properties of soil *New Phytologist* **157** 315-26
- [105] Benard P, Kroener E, Vontobel P, Kaestner A and Carminati A 2016 Water percolation through the root-soil interface *Advances in Water Resources* **95** 190-8
- [106] Read D B, Gregory P J and Bell A E 1999 Physical properties of axenic maize root mucilage *Plant Soil* **211** 87-91
- [107] Bengough Glyn A, Loades K and McKenzie B M 2016 Root hairs aid soil penetration by anchoring the root surface to pore walls *J. Exp. Bot.* **67** 1071-8
- [108] Wilson A J, Robards A W and Goss M J 1977 Effects of mechanical impedance on root growth in barley, *Hordeum vulgare* L.: II. Effects on cell development in seminal roots *J. Exp. Bot.* **28** 1216-27
- [109] Atwell B J 1993 Response of roots to mechanical impedance *Environmental and Experimental Botany* **33** 27-40
- [110] Kuzeja P S, Lintilhac P M and Wei C F 2001 Root elongation against a constant force: experiment with a computerized feedback-controlled device *Journal of Plant Physiology* **158** 673-6
- [111] Barley K P 1965 Effect of localized pressure on growth of maize radicle *Australian Journal of Biological Sciences* **18** 499-&
- [112] Bengough A G 2012 Root elongation is restricted by axial but not by radial pressures: so what happens in field soil? *Plant Soil* **360** 15-8
- [113] Abdalla A M, Hettiaratchi D R and Reece A R 1969 Mechanics of root growth in granular media *J. Agr. Eng. Res.* **14** 236-48
- [114] Hettiaratchi D R P 1990 Soil compaction and plant-root growth *Philosophical Transactions of the Royal Society of London Series B-Biological Sciences* **329** 343-55
- [115] Richards B G and Greacen E L 1986 Mechanical stresses on an expanding cylindrical root analog in antigranulocytes media *Australian Journal of Soil Research* **24** 393-404

- [116] Dorgan K M, Jumars P A, Johnson B, Boudreau B P and Landis E 2005 Burrow extension by crack propagation *Nature* **433** 475
- [117] Dexter A R and Hewitt J S 1978 Deflection of plant roots *J. Agr. Eng. Res.* **23** 17-22
- [118] Chimungu J G, Loades K W and Lynch J P 2015 Root anatomical phenes predict root penetration ability and biomechanical properties in maize (*Zea Mays*) *J. Exp. Bot.* **66** 3151-62
- [119] Wiersum L K 1958 The relationship of the size and structural rigidity of pores to their penetration by roots *Plant Soil* **9** 75-85
- [120] Scholefield D and Hall D M 1985 Constricted growth of grass roots through rigid pores *Plant Soil* **85** 153-62
- [121] Potocka I, Szymanowska-Pulka J, Karczewski J and Nakielski J 2011 Effect of mechanical stress on *Zea* root apex. I. Mechanical stress leads to the switch from closed to open meristem organization *J. Exp. Bot.* **62** 4583-93
- [122] Zwieniecki M A and Newton M 1995 Roots growing in rock fissures - their morphological adaptation *Plant Soil* **172** 181-7
- [123] Taubenhuis J J, Ezekiel W N and Rea H E 1931 Strangulation of cotton roots *Plant Physiol.* **6** 161-6
- [124] Majmudar T S and Behringer R P 2005 Contact force measurements and stress-induced anisotropy in granular materials *Nature* **435** 1079-82
- [125] Radjai F, Jean M, Moreau J J and Roux S 1996 Force distributions in dense two-dimensional granular systems *Physical Review Letters* **77** 274-7
- [126] Radjai F, Roux S and Moreau J J 1999 Contact forces in a granular packing *Chaos* **9** 544-50
- [127] Stone M B, Bernstein D P, Barry R, Pelc M D, Tsui Y K and Schiffer P 2004 Stress propagation: Getting to the bottom of a granular medium - A surprising resistance would be put up by sand grains hiding a buried treasure chest *Nature* **427** 503-4
- [128] Ovarlez G, Kolb E and Clément E 2001 Rheology of a confined granular material *Physical Review E - Statistical, Nonlinear, and Soft Matter Physics* **64** 060302/1-4
- [129] Kolb E, Cixous P, Gaudouen N and Darnige T 2013 Rigid intruder inside a two-dimensional dense granular flow: Drag force and cavity formation *Physical Review E - Statistical, Nonlinear, and Soft Matter Physics* **87**
- [130] Lemaire E, Levitz P, Daccord G and Van Damme H 1991 From viscous fingering to viscoelastic fracturing in colloidal fluids *Physical Review Letters* **67** 2009-12
- [131] Massa G D and Gilroy S 2003 Touch modulates gravity sensing to regulate the growth of primary roots of *Arabidopsis thaliana* *Plant Journal* **33** 435-45
- [132] Silverberg J L, Noar R D, Packer M S, Harrison M J, Henley C L, Cohen I and Gerbode S J 2012 3D imaging and mechanical modeling of helical buckling in *Medicago truncatula* plant roots *Proceedings of the National Academy of Sciences* **109** 16794-9
- [133] Tan T H, Silverberg J L, Floss D S, Harrison M J, Henley C L and Cohen I 2015 How grow-and-switch gravitropism generates root coiling and root waving growth responses in *Medicago truncatula* *Proc. Natl. Acad. Sci. U. S. A.* **112** 12938-43
- [134] Yamanaka T, Nakagawa Y, Mori K, Nakano M, Imamura T, Kataoka H, Terashima A, Iida K, Kojima I, Katagiri T, Shinozaki K and Iida H 2010 MCA1 and MCA2 that mediate Ca²⁺ uptake have distinct and overlapping roles in *Arabidopsis* *Plant Physiol* **152** 1284-96
- [135] Brangwynne C P, MacKintosh F C, Kumar S, Geisse N A, Talbot J, Mahadevan L, Parker K K, Ingber D E and Weitz D A 2006 Microtubules can bear enhanced compressive loads in living cells because of lateral reinforcement *J. Cell Biol.* **173** 733-41
- [136] Chai H 1998 The post-buckling response of a bi-laterally constrained column *J. Mech. Phys. Solids* **46** 1155-81
- [137] Roman B and Pocheau A 2002 Postbuckling of bilaterally constrained rectangular thin plates *J. Mech. Phys. Solids* **50** 2379-401
- [138] Whiteley G M and Dexter A R 1982 Forces required to displace individual particles within beds of similar particles *J. Agr. Eng. Res.* **27** 215-25

- [139] Mojdehi A R, Tavakol B, Royston W, Dillard D A and Holmes D P 2016 Buckling of elastic beams embedded in granular media *Extreme Mech. Lett.* **9** 237-44
- [140] Genet M, Stokes A, Salin F, Mickovski S, Fourcaud T, Dumail J F and van Beek R 2005 The influence of cellulose content on tensile strength in tree roots *Plant Soil* **278** 1-9
- [141] Loades K W, Bengough A G, Bransby M F and Hallett P D 2015 Effect of root age on the biomechanics of seminal and nodal roots of barley (*Hordeum vulgare* L.) in contrasting soil environments *Plant Soil* **395** 253-61
- [142] Mickovski S B, Hallett P D, Bransby M F, Davies M C R, Sonnenberg R and Bengough A G 2009 Mechanical Reinforcement of Soil by Willow Roots: Impacts of Root Properties and Root Failure Mechanism *Soil Sci. Soc. Am. J.* **73** 1276-85
- [143] Whiteley G M and Dexter A R 1981 Elastic response of the roots of field crops *Physiol. Plant.* **51** 407-17
- [144] Forterre Y 2013 Slow, fast and furious: understanding the physics of plant movements *J. Exp. Bot.* **64** 4745-60
- [145] Whiteley G M, Hewitt J S and Dexter A R 1982 The buckling of plant-roots *Physiol. Plant.* **54** 333-42
- [146] Rivière M, Derr J and Douady S 2017 Motions of leaves and stems, from growth to potential use *Physical Biology*
- [147] Migliaccio F and Piconese S 2001 Spiralizations and tropisms in Arabidopsis roots *Trends in Plant Science* **6** 561-5
- [148] Oliva M and Dunand C 2007 Waving and skewing: How gravity and the surface of growth media affect root development in Arabidopsis *New Phytologist* **176** 37-43
- [149] Migliaccio F, Tassone P and Fortunati A 2013 Circumnutation as an autonomous root movement in plants *American Journal of Botany* **100** 4-13
- [150] Stolarz M, Krol E, Dziubinska H and Zawadzki T 2008 Complex relationship between growth and circumnutations in *Helianthus annuus* stem *Plant Signaling and Behavior* **3** 376-80
- [151] Kim H j, Kobayashi A, Fujii N, Miyazawa Y and Takahashi H 2016 Gravitropic response and circumnutation in pea (*Pisum sativum*) seedling roots *Physiol. Plant.* **157** 108-18
- [152] Chen H W, Shao K H and Wang S J 2016 Light-mediated modulation of helix angle and rate of seminal root tip movement determines root morphology of young rice seedlings *Plant Signaling and Behavior* **11**
- [153] Johnsson A 1997 Circumnutations: Results from recent experiments on Earth and in space *Planta* **203** S147-S58
- [154] Bastien R and Meroz Y 2016 The Kinematics of Plant Nutation Reveals a Simple Relation between Curvature and the Orientation of Differential Growth *PLoS Computational Biology* **12**
- [155] Buer C S, Masle J and Wasteneys G O 2000 Growth conditions modulate root-wave phenotypes in Arabidopsis *Plant and Cell Physiology* **41** 1164-70
- [156] Buer C S, Wasteneys G O and Masle J 2003 Ethylene modulates root-wave responses in Arabidopsis *Plant Physiol.* **132** 1085-96
- [157] Simmons C, Soll D and Migliaccio F 1995 Circumnutation and gravitropism cause root waving in Arabidopsis thaliana *J. Exp. Bot.* **46** 143-50
- [158] Kitazawa D, Hatakeda Y, Kamada M, Fujii N, Miyazawa Y, Hoshino A, Iida S, Fukaki H, Morita M T, Tasaka M, Suge H and Takahashi H 2005 Shoot circumnutation and winding movements require gravisensing cells *Proc. Natl. Acad. Sci. U. S. A.* **102** 18742-7
- [159] Thompson M V and Holbrook N M 2004 Root-gel interactions and the root waving behavior of arabidopsis *Plant Physiol.* **135** 1822-37
- [160] Inoue N, Arase T, Hagiwara M, Amano T, Hayashi T and Ikeda R 1999 Ecological significance of root tip rotation for seedling establishment of *Oryza sativa* L *Ecological Research* **14** 31-8
- [161] Ditengou F A, Tealea W D, Kochersperger P, Flittner K A, Kneuper I, van der Graaff E, Nziengui H, Pinosa F, Li X G, Nitschke R, Laux T and Palme K 2008 Mechanical induction of lateral root initiation in Arabidopsis thaliana *Proc. Natl. Acad. Sci. U. S. A.* **105** 18818-23

- [162] Richter G L, Monshausen G B, Krol A and Gilroy S 2009 Mechanical Stimuli Modulate Lateral Root Organogenesis *Plant Physiol.* **151** 1855-66
- [163] Coutand C 2010 Mechanosensing and thigmomorphogenesis, a physiological and biomechanical point of view *Plant Science* **179** 168-82
- [164] Moulia B, Coutand C and Julien J L 2015 Mechanosensitive control of plant growth: Bearing the load, sensing, transducing, and responding *Frontiers in Plant Science* **6**
- [165] Coutand C, Martin L, Leblanc-Fournier N, Decourteix M, Julien J L and Moulia B 2009 Strain mechanosensing quantitatively controls diameter growth and PtaZFP2 gene expression in poplar *Plant Physiol.* **151** 223-32
- [166] Monshausen G B, Bibikova T N, Weisenseel M H and Gilroy S 2009 Ca²⁺ regulates reactive oxygen species production and pH during mechanosensing in arabidopsis roots *Plant Cell* **21** 2341-56
- [167] Peyronnet R, Tran D, Girault T and Frachisse J M 2014 Mechanosensitive channels: Feeling tension in a world under pressure *Frontiers in Plant Science* **5**
- [168] Monshausen G B and Haswell E S 2013 A force of nature: Molecular mechanisms of mechanoperception in plants *J. Exp. Bot.* **64** 4663-80
- [169] Iida H, Furuichi T, Nakano M, Toyota M, Sokabe M and Tatsumi H 2014 New candidates for mechano-sensitive channels potentially involved in gravity sensing in Arabidopsis thaliana *Plant Biology* **16** 39-42
- [170] Hamilton E S, Schlegel A M and Haswell E S 2015 United in diversity: Mechanosensitive ion channels in plants. In: *Annual Review of Plant Biology*, pp 113-37
- [171] Nakagawa Y, Katagiri T, Shinozaki K, Qi Z, Tatsumi H, Furuichi T, Kishigami A, Sokabe M, Kojima I, Sato S, Kato T, Tabata S, Iida K, Terashima A, Nakano M, Ikeda M, Yamanaka T and Iida H 2007 Arabidopsis plasma membrane protein crucial for Ca²⁺ influx and touch sensing in roots *Proc. Natl. Acad. Sci. U. S. A.* **104** 3639-44
- [172] Nakano M, Iida K, Nyunoya H and Iida H 2011 Determination of structural regions important for Ca²⁺ uptake activity in arabidopsis MCA1 and MCA2 expressed in yeast *Plant and Cell Physiology* **52** 1915-30
- [173] Kamano S, Kume S, Iida K, Lei K J, Nakano M, Nakayama Y and Iida H 2015 Transmembrane Topologies of Ca²⁺-permeable Mechanosensitive Channels MCA1 and MCA2 in Arabidopsis thaliana *Journal of Biological Chemistry* **290** 30901-9
- [174] Monshausen G B 2012 Visualizing Ca²⁺ signatures in plants *Current Opinion in Plant Biology* **15** 677-82
- [175] Legué V, Blancaflor E, Wymer C, Perbal G, Fantin D and Gilroy S 1997 Cytoplasmic free Ca²⁺ in arabidopsis roots changes in response to touch but not gravity *Plant Physiol.* **114** 789-800
- [176] Sadeghi A, Tonazzini A, Popova L and Mazzolai B 2014 A Novel Growing Device Inspired by Plant Root Soil Penetration Behaviors *PLoS One* **9** 10
- [177] Sadeghi A, Mondini A, Del Dottore E, Mattoli V, Beccai L, Taccola S, Lucarotti C, Totaro M and Mazzolai B 2017 A plant-inspired robot with soft differential bending capabilities *Bioinspiration & Biomimetics* **12**
- [178] Grossmann G, Guo W J, Ehrhardt D W, Frommer W B, Sit R V, Quake S R and Meier M 2011 The RootChip: An Integrated Microfluidic Chip for Plant Science *Plant Cell* **23** 4234-40
- [179] Stanley C E, Grossmann G, Solvas X C I and deMello A J 2016 Soil-on-a-Chip: microfluidic platforms for environmental organismal studies *Lab Chip* **16** 228-41